Dark *CP* violation and gauged lepton or baryon number for electroweak baryogenesis

Marcela Carena,[1,2,3] Mariano Quirós![],[4] and Yue Zhang![][1,5]

[1]*Theoretical Physics Department, Fermilab, P.O. Box 500, Batavia, Illinois 60510, USA*
[2]*Enrico Fermi Institute, University of Chicago, Chicago, Illinois 60637, USA*
[3]*Kavli Institute for Cosmological Physics, University of Chicago, Chicago, Illinois 60637, USA*
[4]*Institut de Física d'Altes Energies (IFAE), The Barcelona Institute of Science and Technology (BIST), Campus UAB, 08193 Bellaterra (Barcelona) Spain*
[5]*Department of Physics and Astronomy, Northwestern University, Evanston, Illinois 60208, USA*

We explore the generation of the baryon asymmetry in an extension of the standard model where the lepton number is promoted to a $U(1)_\ell$ gauge symmetry with an associated Z' gauge boson. This is based on a novel electroweak baryogenesis mechanism first proposed by us in Ref. [M. Carena, M. Quiros, and Y. Zhang, Electroweak Baryogenesis From Dark *CP* violation, Phys. Rev. Lett. **122,** 201802 (2019).]. Extra fermionic degrees of freedom, including a fermionic dark matter χ, are introduced in the dark sector for anomaly cancellation. The lepton number is spontaneously broken at high scale and the effective theory, containing the standard model, the Z', the fermionic dark matter, and an additional complex scalar field S, violates *CP* in the dark sector. The complex scalar field couples to the Higgs portal and is essential in enabling a strong first order phase transition. Dark *CP* violation is diffused in front of the bubble walls and creates a chiral asymmetry for χ, which in turn creates a chemical potential for the standard model leptons. Weak sphalerons are then in charge of transforming the net lepton charge asymmetry into net baryon number. We explore the model phenomenology related to the leptophilic Z', the dark matter candidate, the Higgs boson, and the additional scalar, as well as implications for electric dipole moments. We also discuss the case when baryon number $U(1)_B$ is promoted to a gauge symmetry, and discuss electroweak baryogenesis and its corresponding phenomenology.

I. INTRODUCTION

The origin of the cosmic baryon asymmetry is a fascinating mystery for particle physics and cosmology. Electroweak baryogenesis (EWBG) [1–5] is an elegant possibility and predicts new physics beyond the standard model (SM), near the electroweak scale, to trigger a sufficiently strong first-order electroweak phase transition (EWPT) and source enough *CP* violation. If the new particles responsible for *CP* violation are charged under the SM, they will also contribute to the electric dipole moments (EDM) at low energies [6]. Models that belong to this class, including two Higgs-doublet models and supersymmetric models, have been progressively receiving stronger and stronger constraints from the improved EDM measurements in recent years [7,8], especially after

the discovery of the Higgs boson [9]. This gives a strong motivation to study EWBG in models with a dark sector where SM gauge singlet particles source the required *CP* violation. The main challenge of such realizations is finding an efficient mechanism to transfer the *CP* violation from the dark sector to the visible sector in the early Universe, while still keeping contributions to EDMs sufficiently suppressed today.

To this respect, an interesting scenario of dark sector *CP* violation was presented in Ref. [10], where a Yukawa interaction between a dark fermion and the SM fermion doublets is responsible for communicating *CP* violation into the visible sector. Such a realization, however, leads to two-loop level contributions to EDMs. In turn, suppressing such contributions to the EDMs requires a finely tuned restoration of a global symmetry after the EWPT.

In a recent short article [11], we presented the basic idea of a new EWBG mechanism in which the role of messenger of the *CP* asymmetry can be played by a Z' gauge boson that couples to both the SM and the dark sector. The low-energy effective theory is a dark sector model containing a Dirac fermion χ (charged under the Z') with a *CP* violating
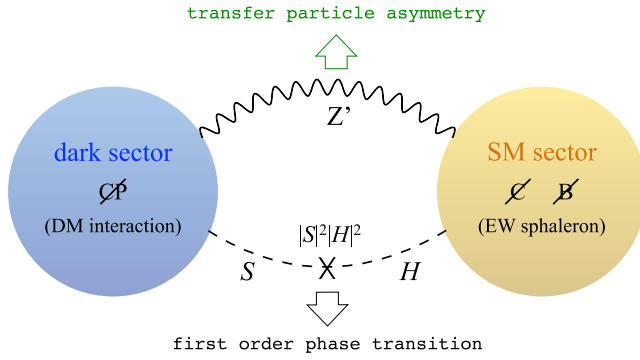
FIG. 1. A schematic picture showing our model setup and the role played by each part in our proposed EWBG mechanism.
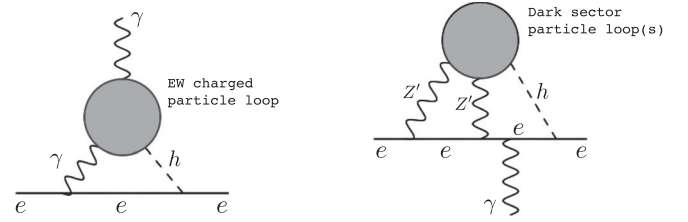

FIG. 2. Representative diagrams showing the loop generated electron EDM in two classes of models, where CP violation occurs through the interactions from electroweak charged particles (left panel) or SM gauge singlets that couple to the Z' (right panel). The gray blobs represent the loop generated $hF_{\mu\nu}F^{\mu\nu}$ and $hZ'_{\mu\nu}Z'^{\mu\nu}$ effective vertices in the two cases, respectively. In the former case, the contribution to EDMs can occur at two-loop level via the Barr-Zee type diagrams. In the latter case, the contribution to EDMs must arise at more than two-loop level.

coupling to a complex scalar field S. During a first-order phase transition, in the electroweak and the dark sectors involving both the Higgs field and the scalar S, a chiral-charge asymmetry in χ particles is first created. Through the timelike component of the Z' background (which is CP odd, and also CPT odd), the χ asymmetry leads to a chemical potential for all SM leptons. If the Z' is sufficiently light, it mediates a long range force that extends into the region outside the bubble wall with unbroken electroweak symmetry. This chemical potential then biases the sphaleron processes and generates a net baryon asymmetry inside the bubbles. After the EWPT is completed, the Z' background relaxes to 0 and the dark CP violation becomes secluded from the SM sector. A schematic plot of this setup is shown in Fig. 1.

There are several distinct features of this model.

(i) The Z' gauge boson needs to be light, not much heavier than the electroweak scale, and not too weakly coupled to the SM leptons, for generating sufficient baryon asymmetry. Therefore, the existence of a light leptophilic Z' serves as a smoking gun of the proposed EWBG mechanism, and provides a well-motivated target for various experimental searches, as we discuss below.

(ii) Given that the CP violating interactions in the dark sector only involve SM gauge singlets, it follows that, in the absence of any Yukawa couplings involving both the SM and the dark sector particles, the two-loop Barr-Zee-type contributions to EDM [12,13] are forbidden. Indeed, we show that in this framework, the leading contribution to EDMs must appear at least at the three-loop level, which is much less constrained by current EDM results. This point is diagrammatically illustrated in Fig. 2.

(iii) The particle χ in this model could serve as the dark matter candidate, as we show in detail in this paper.

(iv) The simple model we have just discussed can be embedded in an ultraviolet (UV) complete theory with gauged lepton number $U(1)_\ell$, whose gauge boson is Z'_μ, for the two interesting benchmark cases,

where $\ell = L_e + L_\mu + L_\tau$ and $\ell = L_\mu + L_\tau$, which require the introduction of extra fermion fields (anomalons) to cancel the gauge anomalies. Below the spontaneous lepton number breaking scale, when part of the anomalon fields have been integrated out, the low-energy effective theory is composed of the SM and a secluded dark sector. The two sectors are connected through the Z', which transfers the CP asymmetry to the observable sector, and the Higgs portal interaction, responsible for inducing a first-order electroweak phase transition.

It is worth noticing that, for our EWBG mechanism to work, the vector current that couples to the Z' boson in the effective theory must be anomalous with respect to the SM $SU(2)_L$ gauge symmetry at the time of the EWPT. This is achieved by (Boltzmann) decoupling the heavy anomalons from the thermal plasma, such that only the SM fields are kept populated at the critical temperature of the EWPT.[1] The effect of the anomalous current is to generate a non-vanishing chemical potential that triggers the electroweak sphaleron processes to create a net baryon asymmetry. The above observation implies that our mechanism will not work, for example, if the Z' is the gauge boson of the $U(1)_{B-L}$ symmetry (anomaly free in the presence of right-handed neutrinos), the hypercharge $U(1)_Y$, or linear combinations thereof. The $U(1)_\ell$ lepton number symmetry we consider is anomaly free at high energy scales, but it becomes anomalous after the spontaneous breaking of the $U(1)_\ell$ gauge symmetry takes place and some of the new fermions—otherwise responsible for anomaly cancellation—are integrated out from the thermal plasma. The effective theory below the mass of the heavy anomalons

---

[1]In other words, while heavy anomalons protect the gauge theory at zero temperature from gauge anomalies, through the remaining Wess-Zumino terms [14], their abundance is Boltzmann suppressed at finite temperature so that they decouple from the thermal bath.

is perfectly consistent, as gauge invariance is restored by the introduction of the Wess-Zumino terms [14]. This is at the core of what makes our baryogenesis mechanism feasible. Similarly, our baryogenesis idea could also work for the gauged $U(1)_B$ baryon number symmetry, which is also known to be anomalous with respect to the SM.

The content of this paper is organized as follows. In Sec. II we present our EWBG model, making explicit the structure of the extended dark fermion and scalar sectors that interact with the SM particles through the $U(1)_\ell$ Z' gauge boson and the Higgs portal. In Sec. III, we discuss the necessary steps for the first-order phase transition to occur, and the source of *CP* violation in the dark sector, as well as how the latter induces the actual mechanism of baryogenesis in the SM at the electroweak scale. In Secs. IV and V we concentrate on the phenomenological aspects of our model and its possible signatures in current and near future experiments, for the cases where $\ell = L_e + L_\mu + L_\tau$ and $\ell = L_\mu + L_\tau$, respectively. This includes the leptophilic Z' searches, dark matter χ direct detection searches, conditions for thermal freeze-out, bounds from EDMs, and collider searches for dark scalar(s). We comment on the case of gauged $U(1)_B$ baryon number in Sec. VI. We reserve Sec. VII for our conclusions and provide some details of the calculation of the lepton asymmetry in Appendixes A and B.

II. A MODEL WITH GAUGED LEPTON NUMBER

As the starting point, we consider an extension of the SM with gauged lepton number symmetry $U(1)_\ell$. Its gauge boson is called Z' and its gauge coupling g'.[2] There are various choices to define the lepton number, ℓ. The most obvious choice is $\ell = L_e + L_\mu + L_\tau$, where all three lepton flavors are gauged universally. However, our baryogenesis mechanism will also work if only a reduced number of lepton flavors are gauged, e.g., $\ell = L_\mu + L_\tau$. In the following discussion, we keep the number of lepton flavors charged under the $U(1)_\ell$ as a free parameter, N_g, where $N_g = 3(2)$ in the case $\ell = L_e + L_\mu + L_\tau (\ell = L_\mu + L_\tau)$.

Because the $U(1)_\ell$ symmetry in the SM is anomalous with respect to $SU(2)_L \times U(1)_Y$, additional fermions (so-called anomalons) must be introduced for anomaly cancellation. A minimal set of new fermion content [15–17] is given in Table I, where q is an arbitrary real number. This is the UV complete framework we consider.

The right-handed neutrinos ν_R^i, $(i = 1, ..., N_g)$ could pair up with the active neutrinos ν_L^i in the SM, so that in this minimal setup the observed neutrino masses are Dirac.[3]

TABLE I. Fermion content (anomalons), and its quantum numbers, in the anomaly-free model with gauged $U(1)_\ell$ symmetry. q is a free (real) parameter.

Particle	$SU(3)_c$	$SU(2)_L$	$U(1)_Y$	$U(1)_\ell$
ν_R^i	1	1	0	1
$L_L' = (\nu_L', e_L')^T$	1	2	$-1/2$	q
e_R'	1	1	-1	q
χ_R	1	1	0	q
$L_R'' = (\nu_R'', e_R'')^T$	1	2	$-1/2$	$q + N_g$
e_L''	1	1	-1	$q + N_g$
χ_L	1	1	0	$q + N_g$

To pair up the other extra fermions and give them vectorlike masses (with respect to the SM gauge symmetries), a complex scalar Φ is introduced carrying lepton number N_g. The vacuum expectation value (VEV) of Φ, v_Φ, spontaneously breaks the $U(1)_\ell$, giving mass to the Z' gauge boson, as

$$M_{Z'} = \sqrt{2} N_g g' v_\Phi, \qquad (2.1)$$

and to the new fermions via the following Yukawa terms:

$$(c_L \bar{L}_R'' L_L' + c_e \bar{e}_L'' e_R' + c_\chi \bar{\chi}_L \chi_R)\Phi + \text{H.c.} \qquad (2.2)$$

Hereafter, for simplicity, we ignore the Yukawa couplings between lepton doublets and singlets with the Higgs boson (which would lead to subleading entries in the fermion mass matrix), as well as the potential Yukawa coupling between the SM leptons and some of the new leptons (only allowed for specific choices of q, for example, q = 1), which also helps to suppress new sources of lepton flavor violation [18].

Because L_L', L_R'', e_R', e_L'' contain fermions charged under the SM gauge group, which are constrained by the existing LEP and LHC searches, we assume v_Φ to be well above the TeV scale and c_L, c_e to be of order 1, rendering these particles sufficiently heavy. As a result, these particles could be integrated out at energy scales and temperatures of order of the $U(1)_\ell$ breaking scale.

For our baryogenesis mechanism to work, we assume both the g' and c_χ parameters to be small, so that the Z' boson, as well as the χ_L, χ_R fermions, have masses around, or even below, the electroweak scale. In the forthcoming discussions, we also show that χ qualifies to be the dark matter candidate.

After integrating out the L_L', L_R'', e_R', e_L'' fermions, which play a role in the anomaly cancellation mechanism, the $U(1)_\ell$ current involving only light degrees of freedom becomes anomalous at lower energy. As it is well known, integrating out the anomalon fields leads to the introduction of the Wess-Zumino (WZ) term [14], which is necessary for restoring the SM gauge invariance when calculating the

---

[2]Not to be confused with the SM hypercharge $U(1)_Y$ gauge coupling, g_Y.

[3]The possibility of Majorana neutrinos is considered in Sec. IV B.

triangle diagrams in the effective theory.[4] However, the coefficient of the WZ term is not fixed but depends on the convention, i.e., the momentum routings, and such convention needs to be respected when calculating the triangle diagrams [19]. In particular, in the convention of "covariant anomaly," the coefficient of the WZ term vanishes [20]. Observe, however, that in the baryogenesis mechanism discussed in this work all the relevant processes occur at tree level, and therefore issues of gauge invariance and appropriate loop momentum convention do not play a role, since they would only matter in one-loop processes involving the Z' (see, e.g., [21]).

In addition to the above particle content, baryogenesis requires the presence of another complex (SM singlet) scalar S, which also carries lepton number N_g. We assume that S is much lighter than Φ, and its VEV v_S evolves, together with that of the Higgs field, during the electroweak phase transition. In contrast, the VEV v_Φ of Φ remains constant as the Universe evolves in the proximity of the electroweak phase transition, since at these scales the field Φ is decoupled. In the presence of the S field, one can write down a Yukawa term that gives an additional mass to the fermion χ. It takes the form

$$\bar{\chi}_L(m_0 + \lambda_c S)\chi_R + \text{H.c.,} \qquad (2.3)$$

where the first term is given by $m_0 = c_\chi v_\Phi$ and λ_c is a (complex) Yukawa coupling. As a result, the mass of χ changes with the S field profile during the electroweak phase transition, and, if the relative phase between m_0 and $\lambda_c S$ is physical, it serves as a source of CP violation in our baryogenesis mechanism.

To summarize, our assumptions lead to a low-energy effective theory below the $U(1)_\ell$ breaking scale (v_Φ), which contains the SM fields plus the following new fields:

$$\boxed{Z'_\mu, \quad S, \quad \chi_L, \quad \chi_R}. \qquad (2.4)$$

Among them, S and $\chi_{L,R}$ are SM gauge singlets and belong to the dark sector. There are two possible portals for them to interact with the SM sector.

One way is through the leptonic Z' portal,

$$\mathcal{L} \supset g' Z'_\mu [(\mathsf{q} + N_g)\bar{\chi}_L \gamma^\mu \chi_L + \mathsf{q}\, \bar{\chi}_R \gamma^\mu \chi_R + \bar{L}_L \gamma^\mu L_L$$
$$+ \bar{\ell}_R \gamma^\mu \ell_R], \qquad (2.5)$$

where L_L represents the SM left-handed lepton doublets and ℓ_R represents the SM right-handed charged leptons. Here, after integrating out the heavy L'_L, L''_R, e'_R, e''_L fermion fields, the Z' couples to an anomalous current with respect to the SM gauge symmetries, in particular, the $SU(2)_L$,

which governs the lepton/baryon number violating sphaleron processes. This is the key ingredient of our baryogenesis mechanism, which makes use of the Z' field background, as we discuss in the following section.

Another way, which is the other key ingredient in our baryogenesis mechanism, is the Higgs portal interaction between S and H,

$$\mathcal{L} = -\lambda_{SH}|S|^2|H|^2, \qquad (2.6)$$

that is responsible for triggering a sufficiently strong first-order electroweak phase transition.

III. ELECTROWEAK BARYOGENESIS MEDIATED BY THE Z' BOSON

In this section we consider how the different ingredients play their roles for successful electroweak baryogenesis. We discuss successively the out of equilibrium condition in the phase transition, the new source of CP violation, and the generation of the baryon asymmetry.

A. The phase transition(s)

We consider a first-order electroweak phase transition during which the Higgs VEV turns on, while the VEV of the S field varies at the same time. Such a scenario can be realized through the following steps in the history of our Universe.

(1) At very high temperatures, all symmetries are restored.

(2) As the Universe cools down to the temperature $T_\Phi \sim v_\Phi$, the Φ field acquires its VEV, $\langle \Phi \rangle = v_\Phi$, and the lepton number symmetry is broken. The nature of this phase transition is not relevant here, but the breaking of lepton number may possibly proceed by a second-order phase transition.

(3) As the Universe further cools down to a temperature T_S not far above the electroweak scale T_{EW}, the S field first develops a VEV, $\langle S \rangle \neq 0$, when its mass squared term (including the thermal corrections) becomes negative, while the Higgs VEV remains 0, $\langle H \rangle = 0$. The transition to this step could be a simple crossover or just a second-order phase transition.

(4) At the critical temperature near the electroweak scale, T_c, a new minimum of the potential with $\langle H \rangle \neq 0, \langle S \rangle \simeq 0$ emerges that turns into the true minimum (replacing the former one with $\langle S \rangle \neq 0$, $\langle H \rangle = 0$). This process must involve a first-order phase transition requiring the presence of a barrier between both minima. The Universe tunnels from one vacuum to the other via bubble nucleation.

A schematic picture of the phase transitions in steps 3 and 4 is depicted in Fig. 3 (left panel). It has been shown [10,22,23] that the above evolutions could be realized

---

[4]A manifestation of the nondecoupling properties of fields that acquire their masses only through a spontaneously breaking mechanism.
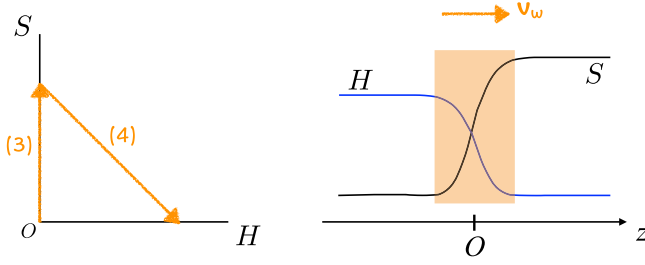
FIG. 3. Schematic plot of the phase transitions. The left plot shows the change of S and H VEVs during steps 3 and 4 discussed in the text. The right plot shows their VEV profiles in front of and behind the expanding bubble wall (shadowed region) during the electroweak phase transition in step 4. The bubble interior is for $z < 0$.

dynamically by the interplay among the terms in the scalar potential describing the Higgs and the new scalar field S. At zero temperature, the scalar potential reads as[5]

$$V(H, S) = \lambda_H(|H|^2 - v^2)^2 + \lambda_S(|S|^2 - v_S^2)^2 + \lambda_{SH}|S|^2|H|^2.$$
(3.1)

The conditions for $H = v$, $S = 0$ to be the global minimum are

$$\lambda_H v^4 > \lambda_S v_S^4, \qquad \lambda_{SH} v^2 > 2\lambda_S v_S^2.$$
(3.2)

At high temperatures, both H and S receive thermal corrections to their quadratic terms, $a_H T^2|H|^2$ and $a_S T^2|S|^2$, with $a_{H,S} > 0$. Thus, at very large T, the potential is minimized for $\langle H \rangle = \langle S \rangle = 0$ (steps 1 and 2). Given that the Higgs field couples to more degrees of freedom than S, it follows that $a_H > a_S$, and it is always possible to find an intermediate temperature where the Higgs quadratic term is positive, while the S quadratic term is negative (step 3), thus triggering a minimum with $\langle S \rangle \neq 0$, $\langle H \rangle = 0$. At lower temperatures, however, the Higgs quadratic term also turns negative. This implies that there should be a critical temperature where the two minima, $(\langle S \rangle \neq 0, \langle H \rangle = 0)$ and $(\langle H \rangle \neq 0, \langle S \rangle = 0)$, are degenerate, allowing for step 4 to occur. The Higgs portal interaction $\lambda_{SH}|S|^2|H|^2$ in Eq. (3.1) [or Eq. (2.6)], which is a cross quartic term, could then provide a tree-level temperature-dependent barrier that separates the two minima allowing for a first-order phase transition. As this phenomenon depends on the particular

---

[5]As the field Φ is integrated out at the electroweak scale, the presence of the Higgs portal terms $\lambda_{\Phi H}|\Phi|^2|H|^2$ and $\lambda_{\Phi S}|\Phi|^2|S|^2$ in (3.1) would amount to a simple redefinition of the mass terms for $|H|^2$ and $|S|^2$, thus not changing the general conclusion that follows. Of course in that case we would have to face a little hierarchy problem, arising from the fact that $v_\Phi \gg v, v_S$, which can be mitigated, e.g., by assuming $\lambda_{\Phi H}, \lambda_{\Phi S} \ll 1$.

values of the potential parameters, we just assume hereafter that they are such that they provide a strong enough first-order phase transition. Detailed model analyses can be found in Refs. [10,22].

B. The source of *CP* violation

The scalar potential, and the χ-S Yukawa coupling terms introduced so far [see Eqs. (3.1) and (2.3)], do not violate *CP* yet. This is because the scalar potential (3.1) is only a function of $|S|$ and, as a result, we are allowed to redefine the argument of S to remove the relative phase between m_0 and $\lambda_c S$ in (2.3). Moreover, any overall phase of the χ mass term can be further removed by redefining the phases of χ_L and χ_R fields. Hence any *CP* violation effect in the Yukawa terms can be absorbed by field redefinitions, leaving no physical effect during the phase transition.

In order to accommodate a physical *CP* violating effect, which is a necessary condition for baryogenesis, one option is to introduce terms in the potential depending on S, which hinders the redefinition of $\arg(S)$. The general form of these terms is

$$\delta V(S) = \rho_S S + \mu_S^2 S^2 + \lambda_{3S}|S|^2 S + \text{H.c.}$$
(3.3)

Naively, these terms violate the $U(1)_\ell$ gauged symmetry and are forbidden in the UV complete theory. However, in this model, one can write renormalizable, $U(1)_\ell$ invariant terms involving Φ and S, as

$$\delta V(\Phi, S) = (\mu_{\Phi S}^2 + \lambda_{\Phi S}|\Phi|^2)\Phi^* S + \lambda'_{\Phi S}\Phi^{*2}S^2$$
$$+ \lambda''_{\Phi S}|S|^2\Phi^* S + \text{H.c.}$$
(3.4)

Clearly, after Φ develops its VEV and the $U(1)_\ell$ symmetry is spontaneously broken, Eq. (3.4) can generate (3.3), leaving the coefficients $\rho_S, \mu_S, \lambda_{3S}$ complex in general. In this discussion, we neglect the backreaction of δV on the VEV of the Φ field, which is a higher order effect in the small v_S/v_Φ expansion.

In the following, for simplicity, we present in more detail the case where only μ_S is nonzero. We could first use the freedom of field redefinition to make the parameters m_0 and μ_S^2 real and positive, but λ_c in general remains as a complex parameter. In this case, $\delta V(S) = 2\mu_S^2|S|^2 \cos[2\arg(S)]$ is the only term in the potential for $\arg(S)$. It is always minimized for $\arg(S) = \pi/2$, such that

$$\delta V(S) = -2\mu_S^2|S|^2.$$
(3.5)

The physical source of *CP* violation arises from the χ mass term, $M_\chi\bar\chi_L\chi_R + M_\chi^*\bar\chi_R\chi_L$, where

$$M_\chi = m_0 + \lambda e^{i\theta}|S|.$$
(3.6)

Here we make the phase of the second term explicit, with $\theta = \arg(\lambda_c) + \pi/2$ and $\lambda \equiv |\lambda_c|$. During a first-order electroweak phase transition, in the presence of a bubble wall, the magnitude of $|S|$ is space-time dependent; hence having used the freedom to make m_0 real, the phase of M_χ is not removable. As is discussed in the following subsection, this phase modifies the dispersion relations of $\chi_{L,R}$, and their antiparticles, in a CP violating way [3], and provides the key source of CP violation for baryogenesis.

When minimizing the potential, we can combine Eq. (3.5) with (3.1) and repeat the discussions in Sec. III A, which still hold with the replacement

$$v_S^2 \to v_S^2 + \frac{\mu_S^2}{\lambda_S}, \qquad (3.7)$$

provided conditions (3.2) hold after the shift (3.7). A special feature of considering only a nonzero μ_S in Eq. (3.3) is that, after the electroweak phase transition, the VEV of S can relax to 0, and the mass of χ today is uniquely determined by m_0.

Alternatively, if the tadpole term $\rho_S S$ is turned on in (3.3), one can still derive the physical CP violating phase similar to (3.6), but the VEV of S after the phase transition remains nonzero. The impact of a nonzero S VEV is only of relevance for the contributions to EDMs, as is discussed in Sec. IV D. So in many of our subsequent discussions we assume, unless explicitly mentioned, that $\rho_S = 0$.

C. The varyogenesis mechanism

In this subsection, we discuss the microscopic particle physics processes for our baryogenesis mechanism to work. All of them happen near the expanding bubble wall, during a first-order electroweak phase transition (step 4 of the early Universe history described in Sec. III A), when the Universe tunnels from the electroweak symmetric vacuum to the broken one via bubble nucleation. Such a phase transition involves the simultaneous changes in the SM Higgs field and the scalar field S. We first rewrite the χ mass term (3.6) with explicit spatial coordinate dependence (labeled by z) in the rest frame of the bubble wall,

$$M_\chi(z) = m_0 + \lambda e^{i\theta} |S(z)|, \qquad (3.8)$$

where z is the distance from the bubble wall, as shown in Fig. 3 (right panel). The $z > 0\,(z < 0)$ region is the electroweak symmetric (broken) phase located outside (inside) the bubble. Our discussion here is in the basis where (m_0, λ, θ) are all real parameters. We parametrize the profile of $|S(z)|$ taking the form

$$|S(z)| = s_0[1 + \kappa \tanh(z/L_w)]/2, \qquad (3.9)$$

where $s_0(1 + \kappa)/2$ is the value of $|S|$ in the electroweak symmetric phase $(z/L_\omega \to \infty)$, and $s_0(1 - \kappa)/2$

parametrizes its value after the completion of the phase transition $(z/L_\omega \to -\infty)$. The bubble wall width and velocity are denoted as L_ω and v_ω, respectively. Here, we focus on the special case $\kappa = 1$ where, after the phase transition (corresponding to $z \ll 0$), the VEV of the S field completely turns off. This can be realized in the presence of the $\mu_S^2 S^2$ term in Eq. (3.3) as discussed above. We expect the qualitative features of our results to hold when the other terms in $\delta V(S)$ are turned on, so that $\kappa \neq 1$.

The phase transition relevant quantities, including the wall width L_ω, the wall velocity v_ω, the scalar field profile across the bubble wall, as well as the critical and nucleation temperatures, T_c and T_n,[6]

We define the particle chiral asymmetries in the dark sector as [3,5], at the nucleation temperature,

$$\xi_{\chi_L}(z) = \frac{3}{T_n^3}(n_{\chi_L} - n_{\chi_L^c}),$$

$$\xi_{\chi_R}(z) = \frac{3}{T_n^3}(n_{\chi_R} - n_{\chi_R^c}), \qquad (3.10)$$

where T_n is the temperature when bubbles emerge, $n_{\chi_{L,R}}$ is the number density of chiral asymmetry, and $\xi_{\chi_{L,R}} T_n \equiv \mu_{\chi_{L,R}}$ defines the corresponding chemical potentials. The Yukawa interaction of $\chi_{L,R}$ with the S background violates CP but preserves a global symmetry $U(1)_\chi$, whose current is defined as $J_\chi^\mu = \bar{\chi}_L \gamma^\mu \chi_L + \bar{\chi}_R \gamma^\mu \chi_R$. As a result, although nonzero values for ξ_{χ_L} and ξ_{χ_R} can be generated by CP violation in the dark sector, the sum $\xi_{\chi_L}(z) + \xi_{\chi_R}(z)$ vanishes. The space-time dependence in the absolute value of the χ mass, $|M_\chi(z)|$, and its phase, $\arg(M_\chi)$, near the bubble wall play an important role by modifying the dispersion relations of $\chi_{L,R}$ particles and their antiparticles in a CP violating way. This affects the phase space distribution of these particles. The resulting chiral asymmetries evolve according to the diffusion equation

$$-D\xi_{\chi_L}'' - v_\omega \xi_{\chi_L}' + \Gamma_m(\xi_{\chi_L} - \xi_{\chi_R}) = S_{\text{CPV}}, \qquad (3.11)$$

---

[6]T_c is defined as the temperature at which the $H = 0$ and $H = v(T_c)$ minima are degenerate, whereas T_n is the temperature at which the phase transition occurs. They are, respectively, all calculable as functions of the model parameters (see, e.g., Ref. [24]). The main goal of this work, however, is to present a new baryogenesis mechanism; hence we leave a detailed study of the strong first-order phase transition, and, in particular, the precise calculation of the value of T_n and the value of the Higgs field at T_n, $v(T_n)$, for a future publication. The detailed analysis of the precise requirements on the model parameters for the phase transition is a straightforward task that however involves computationally intense calculations. In the present work, we assume that the model parameters are such that $v(T_n)/T_n \gtrsim 1$, and we scan over a generous range of T_n values, as well as over other relevant model parameters, including L_ω and v_ω, as shown in Eq. (3.27).
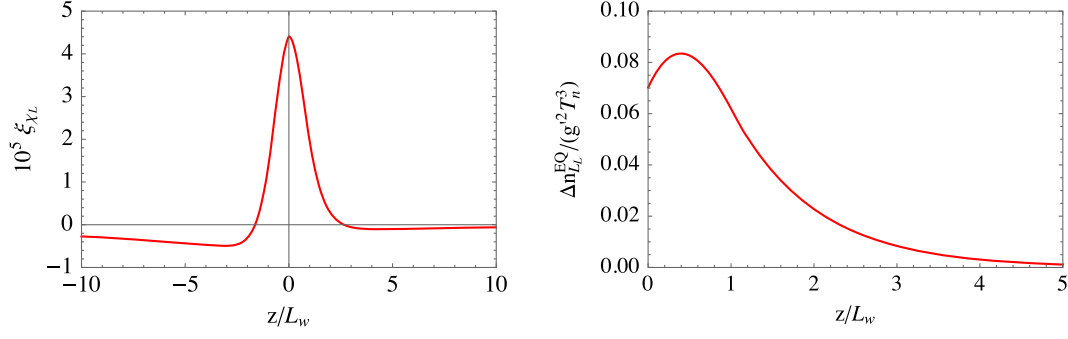
FIG. 4. Left panel: Chiral charge asymmetry in χ_L (opposite for χ_R) particles around the bubble wall, with parameters $m_0 = s_0 = T_n = 100$ GeV, $M_{Z'} = 1$ GeV, $\lambda = 0.3$, $\theta = \pi/3$, $L_\omega = 5/T_n$, $v_\omega = 0.1$. Right panel: $\Delta n_{L_L}^{\mathrm{EQ}}(z)/g'^2 T_n^3$ for the same values of the parameters. For this plot we only show the result in the region $z > 0$ because it corresponds to the range of integrals in Eq. (3.24) or (A4).

where ($'$) means derivative with respect to z. The diffusion constant D is given by $D = \langle v^2 \rangle / (3\Gamma_m)$, with $\Gamma_m \sim \lambda^2 T_n/(4\pi)$, v is the particle velocity in the bubble wall rest frame, and $\langle \rangle$ is the thermal average over the Fermi-Dirac distribution function $f_i(p)$ ($i = \chi_L, \chi_R$) in the rest frame of the bubble wall,

$$f_i(p) = \frac{1}{e^{(E+v_\omega p_z - \mu_i)/T} + 1}, \qquad (3.12)$$

where μ_i is the chemical potential. The corresponding number density for χ_L, χ_R is defined as

$$n_i = \frac{2}{(2\pi)^3} \int d^3 p f_i(p). \qquad (3.13)$$

The *CP* violating source term can be calculated using Refs. [3,5] as

$$
\begin{aligned}
S_{\mathrm{CPV}} &= \frac{v_\omega}{\Gamma_m T_n} \left\langle \frac{v_z}{2E^2} \right\rangle [|M_\chi(z)|^2 (\arg M_\chi(z))']'' \\
&= \frac{v_\omega}{\Gamma_m T_n} \left\langle \frac{v_z}{2E^2} \right\rangle \frac{m_0 s_0 \lambda [-2 + \cosh(\frac{2z}{L_\omega})] \sin\theta}{L_\omega^3 \cosh^4(\frac{z}{L_\omega})},
\end{aligned}
$$
$$(3.14)$$

where $E^2 = p^2 + |M_\chi(z)|^2$.

Clearly, in Eq. (3.11), the source term S_{CPV} must be nonzero in order to generate nonzero asymmetries in the $\chi_{L,R}$ particle numbers, which are proportional to $\xi_{\chi_{L,R}}$, respectively. This requires a nonzero value of $(\arg M_\chi(z))'$; i.e., the phase of the χ mass must *not be* a constant—it has to vary together with the S VEV along the z direction. A quick glance at the form of the χ mass term in Eq. (3.8) shows that m_0 has to be different from 0. We come back to this point near the end of this section when discussing the numerical calculation of the baryon asymmetry and the scan over the parameter space.

The solution to the above diffusion equation is formally given by

$$\xi_{\chi_L}(z) = \int_{-\infty}^{\infty} dz_0 \, G(z - z_0) S_{\mathrm{CPV}}(z_0), \qquad (3.15)$$

where the Green's function $G(z)$ satisfies the equation

$$-DG''(z) - v_\omega G'(z) + 2\Gamma_m G(z) = \delta(z). \qquad (3.16)$$

The solution, continuous at the origin, is given by

$$G(z) = \frac{D^{-1}}{k_+ - k_-} \begin{cases} e^{-k_+ z}, & z \geq 0 \\ e^{-k_- z}, & z < 0 \end{cases},$$

$$k_\pm = \frac{v_\omega}{2D} \left(1 \pm \sqrt{1 + \frac{8\Gamma_m D}{v_\omega^2}} \right). \qquad (3.17)$$

In the left panel of Fig. 4, we show the chiral asymmetry distribution of χ_L as a function of the z coordinate, for a given set of model and phase transition parameters.

Unlike in the usual electroweak baryogenesis scenarios, here the particle chiral charge asymmetry is generated in the dark sector through the χ particle, which is an $SU(2)_L$ singlet and thus does not couple to the electroweak sphalerons. Moreover, for general values of q, the gauge symmetry $U(1)_\ell$ forbids any renormalizable operators through which the asymmetries in χ might be directly shared with the SM fermions that carry the $SU(2)_L$ charge.[7] We here make the observation that, thanks to the leptonic Z' portal, which couples to both χ and the SM leptons, the *CP* violating effect in the dark sector can be transferred in a novel way to the observable sector.

---

[7]As explained in the introduction, this aspect serves as a major difference between our work and that in Ref. [10]. In our case, a new way of transferring the χ particle chiral charge asymmetry to the visible sector is presented.

The main point here is that χ_L and χ_R carry different $U(1)_\ell$ charges ($\mathsf{q} + N_g$ and q, respectively).[8] Consequently, the above chiral asymmetries imply a net $U(1)_\ell$ charge density near the bubble wall as

$$\rho_\ell(z) = (\mathsf{q} + N_g)[n_{\chi_L} - n_{\chi_L^c}] + \mathsf{q}[n_{\chi_R} - n_{\chi_R^c}]$$
$$= \frac{1}{3} N_g T_n^3 \xi_{\chi_L}(z), \tag{3.18}$$

where use has been made of Eq. (3.10). The existence of this net $U(1)_\ell$ charge density yields a Coulomb background of the Z' potential, $\langle Z_0' \rangle$. In the approximation of very large bubbles, this lepton number potential could be calculated in cylindrical coordinates as

$$\langle Z_0'(z) \rangle = \frac{g'}{2M_{Z'}} \int_{-\infty}^{\infty} dz_1 \rho_\ell(z_1) \exp\left[-M_{Z'}|z - z_1|\right], \tag{3.19}$$

where we neglect the impact of $|S(z)|$ on the mass of Z', which is mainly set by the value of v_Φ at a much higher scale.

The background of the vector field Z' breaks the Lorentz symmetry and thus is a *CPT* violating effect, which is also odd under the *CP* transformation. It retains certain similarities to the spontaneous baryogenesis mechanism [25] (also with gravitational baryogenesis [26]), where a time-dependent (*CPT* violating) scalar field couples to the vector current of a particle, and serves as its chemical potential.[9] In our model, we use the timelike component of the Z_μ' gauge boson, whose *CP* and *CPT* violating background is generated due to the microscopic interaction processes between the dark sector particles and the bubble wall described above. The Z_0' background couples to the SM lepton current [see Eq. (2.5)]. As we see, given that this current is anomalous with respect to the SM $SU(2)_L$ gauge symmetry, it could bias the sphaleron process to work in one direction. The Z_0' background then yields a chemical potential for the SM leptons,

$$\mu_{L_L}(z) = \mu_{\ell_R}(z) = g'\langle Z_0'(z) \rangle. \tag{3.20}$$

The thermal equilibrium asymmetry in SM lepton number would then be given by (considering left-handed lepton doublets)

$$\Delta n_{L_L}^{\mathrm{EQ}}(z) = \frac{2N_g T_n^2}{3} \mu_{L_L}(z) = \frac{2g' N_g T_n^2}{3} \langle Z_0'(z) \rangle. \tag{3.21}$$

We show in the right panel of Fig. 4 the spatial distribution of $\Delta n_{L_L}^{\mathrm{EQ}}(z)$ for a given set of model and phase transition parameters. It is worth mentioning that the profiles $\Delta n_{L_L}^{\mathrm{EQ}}(z)$ and $\langle Z_0'(z) \rangle$ depend on our assumption of the bubble profile, Eq. (3.9).

In the presence of the electroweak sphaleron processes, which can change the lepton number, the actual SM lepton number asymmetry evolves toward its equilibrium value. This evolution is governed by the following rate equation,

$$\frac{\partial \Delta n_{L_L}(z,t)}{\partial t} = \Gamma_{\mathrm{sph}}(z - v_\omega t)[\Delta n_{L_L}^{\mathrm{EQ}}(z - v_\omega t) - \Delta n_{L_L}(z,t)],$$
$$\tag{3.22}$$

where Γ_{sph} is the rate for the sphaleron process at the nucleation temperature T_n. The second term on the right-hand side of Eq. (3.22) represents the washout term, which would drive the asymmetry to 0 if the sphaleron processes did not go out of equilibrium quickly enough. Assuming a strong first-order electroweak phase transition, where the condition $v_n/T_n \gtrsim 1$ is fulfilled (v_n is the Higgs VEV at the nucleation temperature T_n), a good approximation for Γ_{sph} is that it is unsuppressed at any point z outside the bubble wall, but becomes exponentially suppressed after the bubble wall has passed through taking this point to the bubble interior, i.e.,

$$\Gamma_{\mathrm{sph}}(z - v_\omega t) = \begin{cases} \Gamma_0 & : \quad t < z/v_\omega \\ \Gamma_0 e^{-M_{\mathrm{sph}}/T_c} & : \quad t > z/v_\omega \end{cases} . \tag{3.23}$$

In Eq. (3.23), $\Gamma_0 \simeq 120\alpha_w^5 T_n \simeq 10^{-6} T_n$ [27], and $M_{\mathrm{sph}} = 4\pi v_n B/g_2$ is the sphaleron mass in the broken phase, where B is a fudge factor [1] that depends on the Higgs mass, and the weak coupling g_2. In the SM, for the experimental value of the Higgs mass it turns out that $B \simeq 1.96$. As discussed in detail in [28], the sphaleron rate in the presence of an additional singlet depends on the parameters in the $V(S, H)$ potential, and could be calculated once this parameter dependence of the first-order phase transition is worked out.

The solution to the rate equation takes the form [3]

$$\Delta n_{L_L} = \frac{\Gamma_0}{v_\omega} \int_0^\infty dz \Delta n_{L_L}^{\mathrm{EQ}}(z) e^{-\Gamma_0 z/v_\omega}. \tag{3.24}$$

We refer the reader to Appendix A for more details on obtaining this result. At this point it is important to realize that the final lepton number density, as given by Eq. (3.24), is nonvanishing as a consequence of the fact that the effective theory at the scale of electroweak baryogenesis has an anomalous lepton number. Had we not integrated out

---

[8]Note, their charges are not chosen by hand but, instead, required by the anomaly cancellation conditions discussed in Sec. II and Table I.

[9]Notice that the VEV of Z_0' vanishes after the electroweak phase transition, as its value stems from the asymmetry in $\chi_{L,R}$ particles, which vanishes when $\arg(M_\chi)$ becomes a constant and the source of *CP* violation S_{CPV} vanishes. Therefore at zero temperature our model does not contain any violation of Lorentz symmetry.

any anomalon propagating in the UV theory, the final lepton number density Δn_L would have been 0. This statement is proven in detail in Appendix B. See also [11].

Because the sphaleron processes preserve $B - L$, equal asymmetries are generated for baryon and lepton numbers, $\Delta n_B = \Delta n_{L_L}$. The entropy density of the Universe at the EW scale is $s \simeq (2\pi^2)g_* T_c^3/45$, where $g_* \simeq g_B + (7/8)g_F \simeq \mathcal{O}(100)$ is the effective number of degrees of freedom at the EW phase transition. The final generated baryon-to-entropy ratio is then

$$\eta_B = \frac{\Delta n_B}{s}. \tag{3.25}$$

The dark blue points in Fig. 5 show the working parameter space where the observed baryon asymmetry [29]

$$\eta_B \simeq 0.9 \times 10^{-10} \tag{3.26}$$

can be generated. They are obtained by scanning over all the model parameters in the following ranges,

$$M_{Z'}, \quad m_0 \in (10^{-3}, 10^3) \text{ GeV}, \quad s_0, \quad T_n \in (100, 500) \text{ GeV}, \quad \lambda \in (10^{-2}, 1),$$
$$g' \in (10^{-6}, 0.1), \quad \theta \in (-\pi/2, \pi/2), \quad L_w \in (1/T_n, 10/T_n), \quad v_\omega \in (0.05, 0.5). \tag{3.27}$$

Here, the parameter m_0 is the mass of the χ particle, assuming S has no VEV today.

We display, in Fig. 5, the baryogenesis viable points in the g' versus $M_{Z'}$ plane assuming $N_g = 3$ (the case $N_g = 2$ is independently exhibited in Sec. V), where the mass parameters satisfy the relation $m_0 > M_{Z'}/2$. The result shows that the smaller the Z' mass, the smaller the value of g' in the allowed region. In particular, with $M_{Z'}$ around 100 MeV, the gauge coupling g' should be as small as 10^{-5}. This feature is expected from the value of the Z'_0 background during baryogenesis, calculated in Eq. (3.19), where parametrically the final baryon asymmetry is proportional to $\sim g'^2/M_{Z'}^2$. In this case, $m_0 > M_{Z'}/2$, the Z' boson

FIG. 5. The parameter space of our model (assuming $N_g = 3$) that could generate the observed baryon asymmetry of the Universe is covered by the blue points, in the g' versus $M_{Z'}$ parameter space. The colorful shaded regions have been excluded by the existing constraints from LEP, *BABAR*, electron $g - 2$, beam dump, and neutrino-electron scattering experiments, as well as the measurement of flavor-changing $K \to \pi$, $B \to K$ decay rates. The yellow band is the favored region for explaining the muon $g - 2$ anomaly. The black dashed line corresponds to the VEV v_Φ equal to 1, 10 TeV. We consider in the parameter scanning the condition $m_0 > M_{Z'}/2$.

is kinematically forbidden to decay into $\chi\bar{\chi}$. If created in the laboratory, it decays into SM particles. This is a visible decay, and in the next section we confront these points with the existing, and near-future, Z' searches. It is worth pointing out that the values of g' of interest for successful baryogenesis are much smaller than 1; thus the backreaction of Z' particles on the bubble wall is negligible.

On the other hand, we find that the resulting points with $m_0 < M_{Z'}/2$ exhibit a different g' versus $M_{Z'}$ correlation behavior. In particular, we find that when the Z' is light (well below the electroweak scale), m_0 is thus small and the required values of g' for successful baryogenesis are much larger (with $g' > 10^{-3}$ everywhere). This could be understood from the explicit expression for the source of CP violation for the baryogenesis mechanism S_{CPV}. As discussed in the paragraph below Eq. (3.12), the relevant CP violation source is proportional to the gradient of $\arg(M_\chi)$ along the z direction, where the VEV of S changes. Clearly, if the m_0 term is very small, $\arg(M_\chi)$ remains approximately θ, and $(\arg(M_\chi))'$ would be suppressed. To compensate for this suppression, larger values of g' are needed. In this case, we find that the experimental constraints from invisibly decaying Z' searches [30] are already strong enough to exclude almost the entire viable parameter space for baryogenesis. Therefore, we do not consider this case any further.
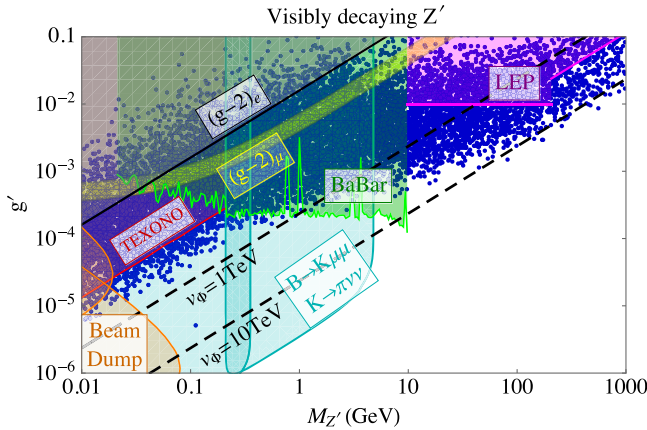
IV. PHENOMENOLOGY

In this section, we discuss the phenomenological consequences of the above-described baryogenesis mechanism. We show that generating the observed baryon asymmetry in the model has a strong impact on the Z' boson search, on the physics of χ as the dark matter candidate, and on the electric dipole moments, as well as on possible LHC signals of the Higgs boson and the dark Higgs S.

Throughout the discussions in this section, we assume the parameter N_g, the number of lepton flavors charged

under the $U(1)_\ell$, to be equal to 3. We comment on the differences in phenomenology if only two lepton flavors are gauged, e.g., $L_\mu + L_\tau$, in the upcoming Sec. V.

A. Searches for the leptophilic Z'

First of all, let us recall that the presence of the Z' boson is the key for the success of our electroweak baryogenesis mechanism. It needs to develop a CP (and CPT) violating background during the electroweak phase transition, which permits transferring the CP violating effect from the dark sector to the SM leptons. In order to generate sufficient final baryon asymmetry, which is proportional to $g'^2/M_{Z'}^2$, the gauge boson Z' cannot be too heavy and the coupling g' should not be too small, as shown in Fig. 5.

At the same time, since the Z' is the gauge boson for the lepton number symmetry, it couples to the SM charged leptons and neutrinos. Such a new vector particle has been directly searched for at e^+e^- colliders, such as LEP (both through resonances [31] and contact interactions [32]) and *BABAR* [33], as well as at electron beam dump experiments [34], and neutrino experiments that are sensitive to neutrino-electron interactions (such as TEXONO) [35]. The Z' could also be exchanged at the loop level and contribute to the anomalous magnetic moments of charged leptons [36]. Many of these constraints are similar to, and could be translated from, the limits on dark photons [35,37]. Because the Z' now mainly couples to charged leptons and neutrinos, we reevaluate its branching ratios based on the following partial decay widths,

$$\Gamma_{Z'\to\ell\bar\ell} = \frac{g'^2}{12\pi} M_{Z'} \left(1 + \frac{2m_\ell^2}{M_{Z'}^2}\right) \sqrt{1 - \frac{4m_\ell^2}{M_{Z'}^2}},$$

$$\Gamma_{Z'\to\nu\bar\nu} = 3 \times \frac{g'^2}{24\pi} M_{Z'}, \qquad (4.1)$$

where $\ell = e$, μ, τ. We neglect the Z' decay into right-handed neutrinos, assuming it is kinematically forbidden.[10] Because the Z' boson in this model is hadrophobic, the constraints from meson decays (π^0, J/Ψ, Υ) into Z' only apply through loop-level processes [35].

Moreover, because the Z' couples to an anomalous current with respect to $SU(2)_L^2$ in the low-energy theory, it makes important contributions to flavor-changing meson decays such as $K \to \pi Z'$ and $B \to K Z'$ through the Wess-Zumino term that occurs at two-loop level [38].[11] For very light Z', these decays are mainly into the longitudinal component of the Z' boson and the corresponding rates are enhanced by $1/M_{Z'}^2$. The Z' boson then decays into charged lepton pairs or neutrinos. Following Ref. [38], we find that

---

[10]The origin of right-handed neutrino masses is addressed in Sec. IV B.
[11]We thank Jeff Dror for pointing out to us the results in Ref. [38].

with these final state stringent limits can be set on the gauge coupling g'.

The existing experimental constraints on a leptophilic Z' are summarized in Fig. 5 for the $N_g = 3$ model. These limits, altogether, set a lower bound on the Z' mass of around 10 GeV. Prospective Higgs factories [39] could explore regions with larger Z' masses.

In addition, the gauge coupling g' is indirectly constrained by requiring the anomalon fields for the $U(1)_\ell$ symmetry to be sufficiently heavy. As discussed in Sec. II, the gauged $U(1)_\ell$ symmetry is broken by the VEV of a scalar field Φ above the electroweak scale. The same VEV defines the mass of the anomalon fields, as a function of their Yukawa coupling. To secure that the anomalon fields are already decoupled during the electroweak phase transition, while avoiding the Yukawa couplings to be in the strongly coupled regime, values of v_Φ above a few times the electroweak scale are required. In Fig. 5, we show indicative values of $v_\Phi = 1$ and 10 TeV, respectively, where we have used the Z' mass given in Eq. (2.1). This shows that most of the experimentally allowed, EWBG-favored solutions are in the region of $M_{Z'}$ above 10 GeV.

Finally we comment that, in general, there is a kinetic mixing between the hypercharge gauge boson B_μ and the new gauge boson Z'_μ, as

$$\mathcal{L}_{\text{kin}} = -\frac{1}{2} c(\mu) F_Y^{\mu\nu} F'_{\mu\nu}, \qquad (4.2)$$

where the coefficient $c(\mu)$ receives renormalization at loop level. Its one-loop beta function takes the form [40]

$$\frac{\partial c(\mu)}{\partial \log \mu} = \frac{g_Y g'}{12\pi^2} \text{Tr}(YL). \qquad (4.3)$$

In the complete UV theory considered here, we have that $\text{Tr}(YL) = -4(\mathsf{q} + 3)$. There is a special case, $\mathsf{q} = -3$, where the kinetic mixing parameter $c(\mu)$ does not run at energies above the $U(1)_\ell$ symmetry breaking scale, v_Φ. For $\mu < v_\Phi$, after integrating out the anomalon fields L'_L, L''_R, e''_L, e'_R, $\text{Tr}(YL) = -6$ in the effective theory. This implies that even if we set $c_{\text{UV}} = 0$ at high scale as the boundary condition, it will be generated at low energies as

$$c(M_Z) \simeq c_{\text{UV}} + \frac{g_Y g'}{2\pi^2} \log \frac{v_\Phi}{M_Z}, \qquad (4.4)$$

where we are assuming that the masses of L'_L, L''_R, e''_L, e'_R are all of order v_Φ, and compute the value of c at the M_Z mass scale where it is measured at the LEP experiment. A nonzero kinetic mixing between B_μ and Z'_μ generates, after electroweak breaking, a mixing between Z_μ and Z'_μ. This could impact LEP observables including the Z boson mass (the ρ parameter), the Z hadronic width, and the forward-backward asymmetries in leptonic Z decays. The analysis in [40] finds that $c(M_Z)$ is constrained to

be less than the percent level, with a much stronger constraint in the region where Z and Z' are nearly degenerate [41]. Compared to the EWBG favored region for g' in Fig. 5, we find it easy to satisfy these constraints provided c_{UV} is small enough.

To summarize, after taking into account all the above constraints, the mass window of the Z' for our baryogenesis mechanism to work is 10 GeV $< M_{Z'} < \mathcal{O}$ (TeV).

B. Neutrino cosmology

It is worth commenting on the neutrino sector of the gauged $U(1)_\ell$ model, and implications of cosmological measurements on additional neutrino degrees of freedom, ΔN_{eff} [29].

As discussed in Sec. II, within the minimal setup, the neutrino mass is Dirac, generated by the Yukawa coupling between the SM active neutrinos ν_{L_i} and the right-handed ones, ν_{R_j}. In the early Universe, at sufficiently high temperatures, the $U(1)_\ell$ gauge interaction could thermalize all ν_{R_i}, and make a contribution to ΔN_{eff} [42]. To avoid an excessive contribution to ΔN_{eff}, one option is to make the $U(1)_\ell$ interaction decouple early enough, preferably above the QCD phase transition temperature, $T_{\text{QCD}} \sim 100$ MeV. The relevant process for thermalizing the ν_R's is $\ell_{\text{SM}} \bar{\ell}_{\text{SM}} \to \nu_{R_i} \bar{\nu}_{R_i}$, through the s-channel Z' exchange, where $\ell_{\text{SM}} = e, \mu, \nu_{L_i}$ are the SM relativistic species, around the T_{QCD} temperature. The corresponding annihilation cross section times relative velocity is

$$\sigma v(\ell_{\text{SM}} \bar{\ell}_{\text{SM}} \to \nu_{R_i} \bar{\nu}_{R_i}) = \frac{g_{\ell_{\text{SM}}} g'^4 s_{\text{CM}}}{48\pi(s_{\text{CM}} - M_{Z'}^2)^2}, \quad (4.5)$$

where $g_e = g_\mu = 2g_{\nu_{L_i}} = 2$, and s_{CM} is the center-of-mass energy squared of the annihilation, of order T^2. The thermal averaged annihilation rate per particle ℓ_{SM}, given by $n_{\ell_{\text{SM}}} \sigma v(\ell_{\text{SM}} \bar{\ell}_{\text{SM}} \to \nu_{R_i} \bar{\nu}_{R_i})$, goes as T^5, in the heavy Z' limit, $M_{Z'} \gg T$. In this case, decoupling ν_R's no later than T_{QCD} amounts to requiring the annihilation rate to be less than the Hubble expansion rate at T_{QCD}. This in turn implies that

$$v_\Phi \gtrsim 10 \text{ TeV}, \quad \text{for } M_{Z'} \gg T_{\text{QCD}}. \quad (4.6)$$

On the other hand, if $M_{Z'} \ll T_{\text{QCD}}$, the thermal averaged annihilation rate scales as T until the temperature falls below the Z' mass. In this case, requiring that ν_{R_i} never reaches thermal equilibrium implies that

$$g' \lesssim 10^{-5}\left(\frac{M_{Z'}}{1 \text{ MeV}}\right)^{1/4}, \quad \text{for } M_{Z'} \ll T_{\text{QCD}}. \quad (4.7)$$

Satisfying conditions (4.6) and (4.7) imposes strong constraints on the EWBG viable parameter space found

in Fig. 5. See [43] for a recent calculation in a similar context.

The viable alternative option for neutrino mass is to implement the seesaw mechanism by giving Majorana masses to ν_{R_i}. If all the ν_{R_i} are heavier than ~ 500 MeV, they decay before the big bang nucleosynthesis and have no effect in ΔN_{eff} [44]. However this option requires extending the scalar sector of the model by introducing an extra SM singlet Φ' with lepton number $L = 2$, which couples to the right-handed neutrinos as

$$\sum_{\alpha,\beta=e,\mu,\tau} Y'_{\alpha\beta} \bar{\Phi}' \bar{\nu}_{R\alpha}^c \nu_{R\beta} + \text{H.c.} \quad (4.8)$$

For large enough values of $v_{\Phi'} \gtrsim 100$ GeV, the new scalars from the Φ' field could kinematically evade searches at LEP. Note, on the other hand, that we need $v_{\Phi'} \ll v_\Phi \sim$ TeV in order not to perturb the results of this paper on electroweak baryogenesis. However, this requires a more detailed study of the effects on the nature of the electroweak phase transition. The experimental search for heavy Majorana neutrinos is of great phenomenological interest [45], especially as the $U(1)_\ell$ gauge interaction here opens a new production channel for them. We investigate this exciting opportunity in a future work.

C. χ as dark matter

As mentioned earlier, in this model, the particle χ from the dark sector could be a dark matter candidate, since there is a $\mathbb{Z}_2$ symmetry in the Lagrangian ($\chi \to -\chi$) allowing it to be stable.

1. The thermal relic density

If the VEV of S relaxes to 0 after the electroweak phase transition, the mass of χ is given by m_0. From the above baryogenesis analysis point of view, we find that χ is favored to be heavier than Z' (see Fig. 5 and corresponding discussions). In the following, we consider all the possible annihilation channels, as shown in the first row of Fig. 6, that will contribute to the dark matter relic density.

Let us first consider the annihilation channel $\chi\bar{\chi} \to Z'Z'$ (upper-left diagram of Fig. 6). The annihilation cross section is [46]

$$(\sigma v_{\text{rel}})_{\chi\bar{\chi} \to Z'Z'}$$

$$= \frac{g'^4}{64\pi M_{Z'}^2} \frac{\left(1 - \frac{M_{Z'}^2}{m_0^2}\right)^{3/2}}{\left(1 - \frac{M_{Z'}^2}{2m_0^2}\right)^2}$$

$$\times \left[18(2\mathsf{q} + 3)^2 + \frac{M_{Z'}^2}{m_0^2}(2\mathsf{q}^2 - 9)(2\mathsf{q}^2 + 12\mathsf{q} + 9)\right]$$

$$\xrightarrow{m_0 \gg M_{Z'}} \frac{9g'^4(2\mathsf{q} + 3)^2}{32\pi M_{Z'}^2}, \quad (4.9)$$
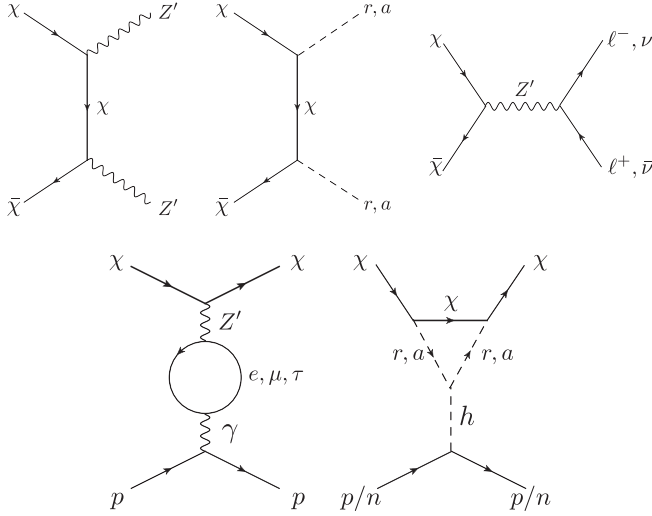
FIG. 6. Feynman diagrams for dark matter thermal freeze-out (first row) and direct detection (second row) in the model we consider. Time flows from left to right.

where $v_{\rm rel}$ is the relative velocity between χ and $\bar{\chi}$ particles before the annihilation, and in the last step we take the limit that $m_0 \gg M_{Z'}$. Requiring that χ obtains the observed relic abundance [29] through this annihilation mechanism, we get

$$g' \simeq \sqrt{\frac{M_{Z'}}{5.9~{\rm TeV} \times |2{\sf q} + 3|}}. \qquad (4.10)$$

This relation is shown by the red curve in Fig. 7 (left panel), for a particular value of ${\sf q} = -3$ (similar results hold for other values of ${\sf q}$, as long as ${\sf q}$ is of order 1). Comparing with the blue and magenta dots, which are the phenomenologically allowed points for successful baryogenesis (surviving the various constraints in Fig. 5), we find these values of g' are too small to account for the correct dark matter relic density this way, unless the dark matter charge ${\sf q}$ value is unnaturally large. Hence, we need larger contributions to the dark matter annihilation cross section from additional channels.

Next, we consider the s-channel Z' exchange, as shown by Fig. 6 (upper-right diagram), where $\chi\bar{\chi}$ annihilate into SM charged leptons and neutrinos. The corresponding cross section is (assuming the limit $m_0 \gg M_{Z'}$)

$$(\sigma v_{\rm rel})_{\chi\bar{\chi} \to \ell^+ \ell^-, \nu\bar{\nu}} = \frac{9g'^4(2{\sf q} + 3)^2}{128\pi m_0^2}. \qquad (4.11)$$

Comparing this expression with Eq. (4.9), we find that $(\sigma v_{\rm rel})_{\chi\bar{\chi} \to \ell^+ \ell^-, \nu\bar{\nu}}$ is not sufficiently large, since it is parametrically smaller than $(\sigma v_{\rm rel})_{\chi\bar{\chi} \to Z'Z'}$, for $m_0 \gg M_{Z'}$. The latter having an enhancement factor, $m_0^2/M_{Z'}^2$, which arises from $\chi\bar{\chi}$ mainly annihilating into the longitudinal component of the Z' boson.

Finally, we consider the dark matter annihilation into the dark scalar S. Here we first derive the dark scalar spectrum and its couplings to the dark matter χ. The most general scalar potential of S is given by the sum of Eqs. (3.1) and (3.3). We focus on the case where in (3.3) only the
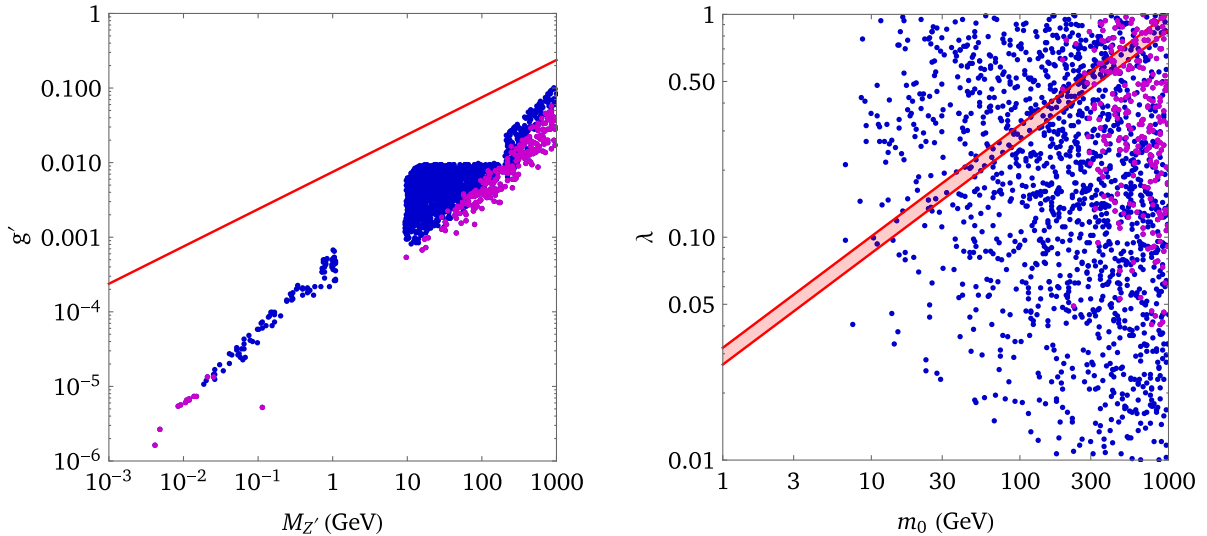

FIG. 7. Confronting the electroweak baryogenesis favored parameter space (shown by the blue and magenta points) with dark matter observables, assuming the χ particle, which sources CP violation in baryogenesis, is also the dark matter candidate. All the blue and magenta points in the plots satisfy the constraints on the Z' boson shown in Fig. 5. The magenta points are consistent with both the observed baryon asymmetry and the dark matter direct detection experiments, while the blue points fail to pass the latter constraint. In the left (right) panel, on the red curve (band), the χ particle could explain the correct relic density through the thermal freeze-out mechanism via the annihilation channel $\chi\bar{\chi} \to Z'Z'$ ($\chi\bar{\chi} \to rr, aa, ra$).

quadratic term $\mu_S^2 S^2 + \text{H.c.}$ is present, and the VEV of S relaxes to 0 when the dark matter freezes out (which typically occurs at temperatures below the electroweak phase transition). In this case, CP can be violated in the dark sector as explained in Sec. III B. We can first redefine the phases of S and $\chi_{L,R}$ fields so that m_0 and μ_S are real parameters, but the λ_c coupling in Eq. (2.3) remains complex in general. As before, we rewrite $\lambda_c = \lambda e^{i\theta_\lambda}$ with λ and θ_λ being real parameters. In this basis, the complex scalar S is separated into its real and imaginary parts $S = (r + ia)/\sqrt{2}$, where r and a are the physical mass eigenstates, with respective masses

$$M_r^2 = \lambda_{SH} v^2 - 2\lambda_S v_S^2 + 2\mu_S^2,$$
$$M_a^2 = \lambda_{SH} v^2 - 2\lambda_S v_S^2 - 2\mu_S^2. \qquad (4.12)$$

Conditions (3.2) and (3.7) guarantee that both M_r^2 and M_a^2 are positive. Clearly, the presence of the $\mu_S^2 S^2 + \text{H.c.}$ potential term breaks the degeneracy between r and a, $M_r \neq M_a$. It is then straightforward to rewrite the Yukawa interaction, Eq. (2.3), into those between r, a and the fermion χ, which takes the form

$$\mathcal{L}_{\text{dark Yukawa}} = \lambda e^{i\theta_\lambda} \bar{\chi}_L \chi_R S + \text{H.c.}$$
$$= \frac{r}{\sqrt{2}} (\lambda \cos\theta_\lambda \bar{\chi}\chi + \lambda \sin\theta_\lambda \bar{\chi} i\gamma_5 \chi)$$
$$+ \frac{a}{\sqrt{2}} (-\lambda \sin\theta_\lambda \bar{\chi}\chi + \lambda \cos\theta_\lambda \bar{\chi} i\gamma_5 \chi). \quad (4.13)$$

With these interactions, we calculate the cross sections for $\chi\bar{\chi}$ annihilating into rr, aa, and ra. The corresponding Feynman diagrams are shown in Fig. 6 (upper-middle diagram). The sum of these annihilation cross sections is

$$(\sigma v_{\text{rel}})_{\chi\bar{\chi}\to rr} + (\sigma v_{\text{rel}})_{\chi\bar{\chi}\to aa} + (\sigma v_{\text{rel}})_{\chi\bar{\chi}\to ra} \simeq \frac{\lambda^4 (3 - \cos 4\theta_\lambda)}{256\pi m_0^2},$$
$$(4.14)$$

where we assume that the final state particles r and a are much lighter than χ. Obtaining the correct relic density for χ through this channel then requires λ to lie within the window

$$\sqrt{\frac{m_0}{1.4 \text{ TeV}}} < \lambda < \sqrt{\frac{m_0}{1.0 \text{ TeV}}} \qquad (4.15)$$

for $0 < \theta_\lambda < 2\pi$. This relation is derived by assuming that the $\chi\bar{\chi} \to Z'Z'$ and $\chi\bar{\chi} \to \ell^+\ell^-, \nu\bar{\nu}$ annihilation cross sections discussed above are much smaller than the one in Eq. (4.14), and thus negligible when accounting for the total value of the thermal relic density. Region (4.15) is shown by the red band in Fig. 7 (right panel). Again, the blue/magenta dots are the phenomenologically viable

points obtained from the baryogenesis scan, and now shown in the λ versus m_0 parameter space. This comparison makes it clear that there exists a viable region in the parameter space where both successful electroweak baryogenesis and correct dark matter relic density are achievable. The favored region of dark matter mass is around a few hundred GeV.

2. The direct detection

Direct detection of dark matter in this model could occur through Z' exchange. However, because the Z' is the gauge boson for lepton number, it does not directly couple to nucleons, implying that the dark matter-nucleon scattering should occur through the loop of charged leptons that effectively act as a kinetic mixing between the Z' and the photon, as shown in Fig. 6 (lower-left diagram). The corresponding spin-independent cross section for this process is [47]

$$\sigma_{\chi p \to \chi p} = \frac{16\alpha^2 \alpha'^2 (\mathsf{q} + 3/2)^2 \mu_p^2}{81\pi (q^2 - M_{Z'}^2)^2} \left[\sum_{\ell=e,\mu,\tau} f(q^2, m_\ell) \right]^2,$$
$$(4.16)$$

where $\alpha' = g'^2/(4\pi)$, $\mu_p = m_0 m_p/(m_0 + m_p)$ is the reduced mass of the dark matter and target nucleus system (m_p is the proton mass), and

$$f(q^2, m_\ell) = \frac{1}{q^2} \left[5q^2 + 12m_\ell^2 + 6(q^2 + 2m_\ell^2)\sqrt{1 - \frac{4m_\ell^2}{q^2}} \right.$$
$$\left. \times \operatorname{arccoth}\left(\sqrt{1 - \frac{4m_\ell^2}{q^2}} \right) + 3q^2 \log\frac{\Lambda^2}{m_\ell^2} \right],$$
$$(4.17)$$

where Λ is the cutoff scale corresponding to the renormalization of the effective $Z' - \gamma$ kinetic mixing. We set $\Lambda = 1$ TeV in our calculation, and assume $\mathsf{q} \sim O(1)$. The typical square momentum transfer of the scattering is of order $q^2 = -4\mu^2 v^2$, where $v \simeq 10^{-3}$ is the typical halo dark matter velocity.[12] In Fig. 7, the points in magenta are compatible with the present dark matter direct detection constraints [48], and can generate the observed baryon asymmetry in the Universe.

In addition, the dark matter direct detection could also be mediated by the scalar S (or equivalently the r, a mass eigenstates) and the Higgs boson exchange. If S has no VEV today, the dark matter scattering is a loop-level process, as shown in Fig. 6 (lower-right diagram). In this case, the cross section arises from a loop suppressed Higgs

---

[12]In the case of the xenon nucleus target, we have $\mu = m_0 m_{\text{Xe}}/(m_0 + m_{\text{Xe}})$, with $m_{\text{Xe}} \sim 130 m_p$.
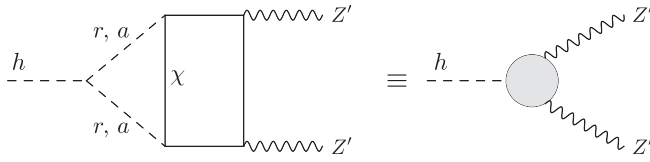
FIG. 8.   Two-loop generated $hZ'_{\mu\nu}\tilde{Z}'^{\mu\nu}$ vertex.

portal interaction and is sufficiently small and can be neglected [49]. On the other hand, if S were to have a nonzero VEV, it would mix with the Higgs boson and the dark matter scattering would occur at tree level. In such a case, the direct detection constraints could become important depending on the mass of S and the size of its mixing with the Higgs boson [50].

D. Implications for electric dipole moments

We comment here on the implications of our baryogenesis model for the electric dipole moment experiments. It is generically expected that the CP violating interaction between S and χ, required for successful baryogenesis, will propagate at loop level to the standard model sector, giving rise to EDMs.

The relevant interaction and mass terms for CP violation in the dark sector are given in Eqs. (2.3) and (3.3). We first consider the case where the VEV of S at zero temperature is 0 and only the $\mu_S^2 S^2 + \text{H.c.}$ term is present in Eq. (3.3). As explained in Sec. IV C 1, the complex scalar S splits into its real and imaginary parts, yielding the physical mass eigenstates, r and a, respectively, and their interactions with dark matter are given by Eq. (4.13). If $\theta_\lambda \neq 0$, the r and a fields couple to both scalar ($\bar{\chi}\chi$) and pseudoscalar ($\bar{\chi}i\gamma_5\chi$) operators involving the χ fields. At the same time, they also couple to the SM Higgs boson through the Higgs portal interaction, Eq. (2.6),

$$\lambda_{SH}|S|^2|H|^2 \supset \frac{\lambda_{SH}v}{2}h(r^2 + a^2). \tag{4.18}$$

Then Eqs. (4.13) and (4.18) allow us to derive a CP violating Higgs-Z' operator, of the form $hZ'_{\mu\nu}\tilde{Z}'^{\mu\nu}$, at two-loop level, as shown in Fig. 8. Out of the two vertices where the dark scalars (r or a) are attached to the χ loop, one of them needs to be the scalar coupling in Eq. (4.13) and the other the pseudoscalar coupling, so that CP can be violated. The resulting coefficient of the $hZ'_{\mu\nu}\tilde{Z}'^{\mu\nu}$ operator is proportional to $\lambda^2 \sin\theta_\lambda \cos\theta_\lambda$.

It is worth noting that the nondegeneracy between r and a is the key for the coefficient of this operator to be nonzero; otherwise the coupling structure in (4.13) would lead to a complete cancellation between the two diagrams involving r and a, respectively. This cancellation could also be understood from a symmetry argument. Based on the discussions in Sec. III B, if the δV potential (containing $\mu_S^2 S^2$ term) vanishes, thus leading to degenerate r and a
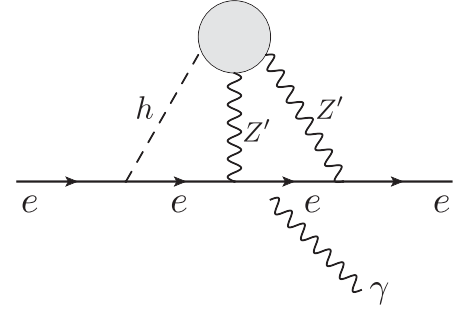

FIG. 9.   Two-loop generated electron EDM, from the $hZ'_{\mu\nu}\tilde{Z}'^{\mu\nu}$ vertex (represented by the gray blob). In our model, the $hZ'_{\mu\nu}\tilde{Z}'^{\mu\nu}$ is generated at two-loop level; see Fig. 8. The photon must be radiated from one of the internal propagators and that has to be an electron propagator because everybody else is electrically neutral.

fields, there is no CP violation in the dark sector—all the parameters can be made real by field redefinitions—and there is no contribution to any CP violating operators.

In the presence of dark sector CP violation, when the contribution to the $hZ'_{\mu\nu}\tilde{Z}'^{\mu\nu}$ operator is nonzero, we could use it to further generate the EDM for the electron, at the price of another two loops, as shown in Fig. 9. Unlike the Barr-Zee-type diagrams for EDMs [12], here we must attach both Z' s to the electron line and the external photon to either of the internal electron propagators.

By simple power counting, the resulting electron EDM is

$$d_e \sim \frac{eG_F m_e}{(16\pi^2)^4} (\lambda_{SH}\lambda^2 g'^4 \mathsf{q}^2) \sin(2\theta_\lambda)$$
$$\lesssim 10^{-30} (\lambda_{SH}\lambda^2 g'^4 \mathsf{q}^2) \sin(2\theta_\lambda) e \text{ cm}. \tag{4.19}$$

This estimate is valid assuming that the r and a mass difference is around the electroweak scale. With the factor $(\lambda_{SH}\lambda^2 g'^4 \mathsf{q}^2) < 1$, the resulting electron EDM is well below the current upper bound on d_e, which comes from the ACME experiment [7]: $d_e < 1.1 \times 10^{-29} e$ cm. As mentioned in the introduction, this is an appealing feature of our model for electroweak baryogenesis that, unlike many others, is safe from the EDM constraints, even if the CP phase is of order 1.

Finally, we comment on the case where the VEV of S at zero temperature is nonzero. In this case, from the Higgs portal interaction, Eq. (2.6), there is a direct mixing between r and h fields. As a result, the $hZ'_{\mu\nu}\tilde{Z}'^{\mu\nu}$ vertex could be generated by replacing the scalar loo in Fig. 8 by the $r - h$ mixing, with only one r attached to the fermion loop via the pseudoscalar coupling, which becomes a one-loop diagram. The contribution to the electron EDM in this case reduces to three loops,

$$d_e \sim 10^{-28} (\lambda_{SH}v v_S/M_r^2) \sin\theta_\lambda e \text{ cm}, \tag{4.20}$$

where the factor $(\lambda_{SH}v v_S/M_r^2)$ is the mixing between r and h. The Higgs boson rate measurements at the LHC requires
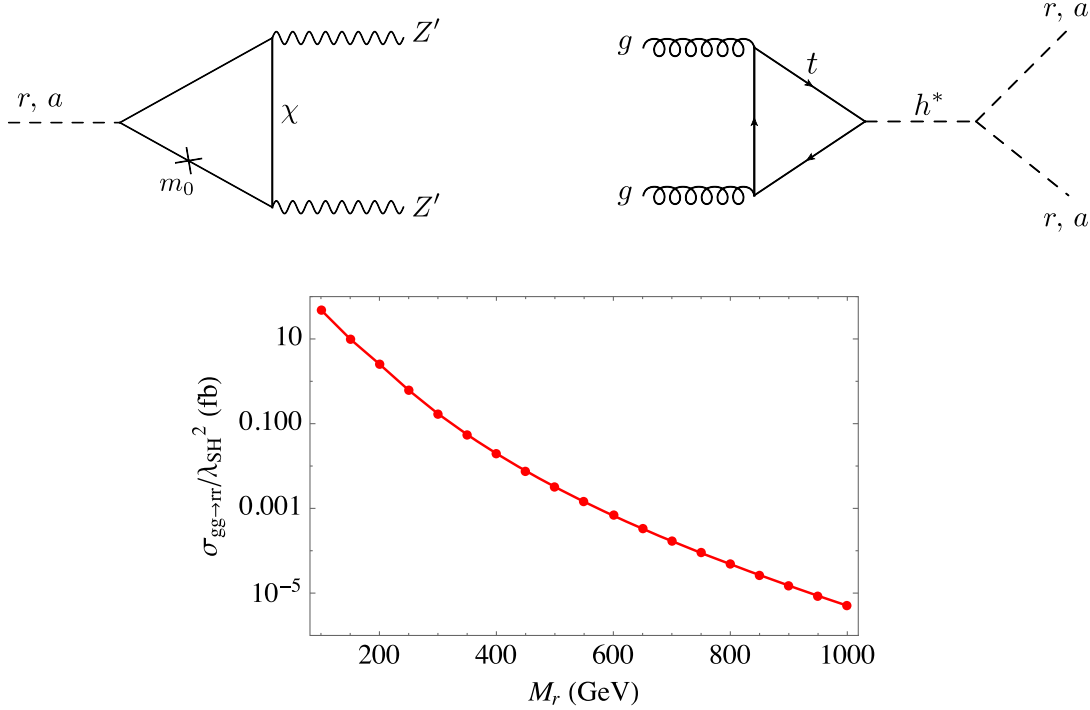
FIG. 10. Feynman diagrams for the loop induced decay of r, a into two Z' bosons (upper left) and the production process $gg \to rr$ (or aa) via an off-shell Higgs boson (upper right). The cross section for the latter at $\sqrt{s} = 13$ TeV LHC is shown in the lower panel.

this mixing must to be less than $\lesssim 20\%$ [51]. This implies that $d_e \lesssim 10^{-29} \sin\theta_\lambda e$ cm, allowing the predicted EDM to be closer to the current upper bound and giving a prospect for future electron EDM searches.

E. Possible LHC signals of the dark scalar(s)

In this subsection, we comment on the possible collider signals of the new scalar S in our model. Unlike the electroweak phase transition discussion, where only the S field background is relevant, here we consider the S excitations, being produced as particles. As mentioned in Sec. IV D, the physical states from the S field are its real, r, and imaginary, a, parts, which have different masses. Their interactions with χ are given by Eq. (4.13); thus, if kinematically allowed, they could dominantly decay into $\chi\bar{\chi}$. However, as discussed in Sec. IV C, for the dark matter χ to freeze out effectively we need r and a to be lighter than χ. In this case, they have to decay via a loop of χ into a pair of Z' bosons, as shown in Fig. 10 (upper left panel).[13] This could lead to a potentially interesting signature because the Z' boson, which is typically lighter than χ (necessary for successful baryogenesis), has to decay into SM charged leptons or neutrinos. Each decaying r or a could then produce as many as four charged leptons.

There is important information about the model in these charged lepton decay products. First, each pair of the

charged leptons sits on the Z' resonance, so their invariant masses all line up in the same energy bin corresponding to the Z' mass. Moreover, because r (and a) has both *CP* even and odd couplings with χ, the effective operators for its decay (after integrating out χ in the loop) are $r Z'_{\mu\nu} Z'^{\mu\nu}$ and $r Z'_{\mu\nu} \tilde{Z}'^{\mu\nu}$. The interference of the two decay amplitudes allows us to probe *CP* violating observables in the final state charged lepton angular distributions, in analogy to using the golden channel of the Higgs decay to probe *CP* violation [52].

For the production of the new scalars r, a, we resort to the Higgs portal interaction, Eq. (2.6) or (4.18). If the S field has no VEV today, there is a $\mathbb{Z}_2$ symmetry at this vertex that requires that r or a must be pair produced. This may occur at the LHC, or a prospective future hadron collider, through the gluon fusion process that creates an off-shell Higgs boson, which later on splits into two r (or a) particles, as shown in Fig. 10 (upper right panel). The corresponding production cross section at the LHC is shown in the lower panel of Fig. 10. Quantitatively, $\sigma_{gg \to rr, aa} \sim 10\lambda_{SH}^2$ fb ($\sim 0.1\lambda_{SH}^2$ fb) for $M_{r,a} \simeq 150$ GeV (for $M_{r,a} \simeq 300$ GeV). After the decays of the r (or a) scalars, the final state could contain as many as four pairs of charged leptons, which would provide a very striking signal. A recent analysis [53] has shown that the multi-lepton final state data from the LHC [54] could already set useful limits on dark sector models. Comparing the production cross section shown in Fig. 10 with the limits derived in [53], we find that the existing LHC data could

---

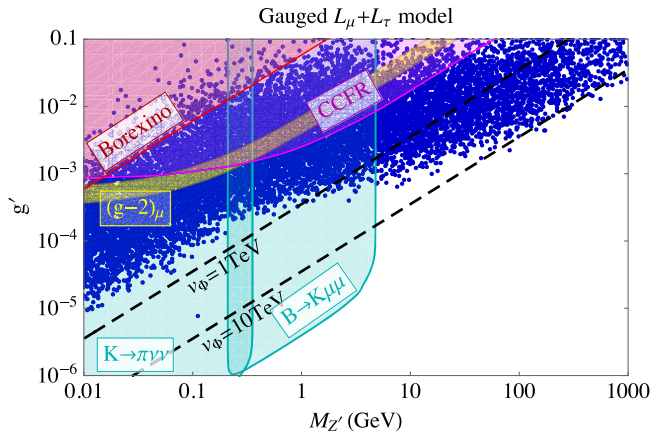[13]A similar diagram makes in the standard model the "golden channel" decay $h \to \gamma\gamma$ via a top quark loop.

FIG. 11. Scanned points (blue) in the $g'-M_{Z'}$ plane, compatible with the observed baryon asymmetry of the Universe assuming $N_g = 2$. The colorful shaded regions have been excluded by the existing constraints from the CCFR, Borexino experiments, and the $K \to \pi \nu \bar{\nu}$ and $B \to K \mu \mu$ decay rate measurements, respectively. The yellow band is the favored region for explaining the muon $g - 2$ anomaly. The black dashed lines corresponding to v_Φ equal 1 and 10 TeV, two indicative values related to the anomalon masses that need to be above the electroweak scale.

already cover the region where the dark scalar (r or a) is lighter ~ 200 GeV for $\lambda_{SH} \sim \mathcal{O}(1)$.

Finally, we comment on the case where S has a nonzero VEV today. A nonzero VEV of S allows r-Higgs boson mixing implying that, in addition to the above pair production mode, r may be singly produced through mixing via the gluon fusion channel. There are two possibilities to consider: (a) the Higgs boson is produced off shell and subsequently mixes with r, that is, produced on shell as a new resonance and decays to a Z' pair at tree level, leading to four leptons in the final state. This is an interesting signature to be explored. The new r resonance can also decay to SM final states, but this is further suppressed by an additional $r - h$ mixing factor. (b) The Higgs boson can be produced on shell and its decays can be modified through its mixing with r. Importantly, this has a direct impact on precision measurements of the SM-like Higgs boson, by modifying the Higgs couplings to SM particles, allowing for Higgs exotic decays, and affecting the di-Higgs production rate. In particular, the current bound [55] on Higgs exotic decay $h \to 2Z' \to 4\ell$ is consistent with an order 1 $r - h$ mixing, for $g' \lesssim 10^{-2}$ and $v_S \lesssim 100$ GeV. This region of parameter space is just below the LEP bound shown in Fig. 5 and is an interesting benchmark for future collider searches.

V. THE CASE OF GAUGED $L_\mu + L_\tau$

In this section, we consider another incarnation of the gauged $U(1)_\ell$ model where only two lepton flavors are gauged, $\ell = L_\mu + L_\tau$, $N_g = 2$. We comment on the

differences and similarities for the EWBG predictions, as well as the phenomenological implications between this two flavor case and the previously studied three flavor case with $\ell = L_e + L_\mu + L_\tau$.

The previous discussion on our recently proposed EWBG mechanism in Sec. III has assumed a generic value of N_g. The parametric dependence of the final baryon asymmetry to entropy ratio is given by

$$\eta_B = \frac{\Delta n_B}{s} \propto \frac{g'^2 N_g^2 T_c^3 L_\omega \alpha_W^5}{M_{Z'}^2 v_\omega}, \qquad (5.1)$$

from where one observes that, for a fixed value of $M_{Z'}$, it scales as $g'^2 N_g^2$; i.e., the favored values of g' in the $N_g = 2$ case are ~ 1.5 times larger than those in the $N_g = 3$ case. In Fig. 11, the blue points show the EWBG-favored region of parameter space in the g' versus $M_{Z'}$ plane, obtained by scanning over the model and phase transition parameters given by Eq. (3.27). This figure is analogous to Fig. 5 for the $N_g = 2$ case.

Experimentally, the gauged $L_\mu + L_\tau$ model is interesting because the Z' does not couple to electrons at tree level. This helps to avoid most constraints discussed in Sec. IVA. There are, however, relevant constraints from neutrino trident production (CCFR) [56] and loop-induced solar-neutrino-electron scattering (Borexino) [35,57] that exclude the correspondingly labeled shaded regions in Fig. 11. In this model, the Borexino experiment stands out to be the most important neutrino scattering experiment because the solar neutrino contains a ν_μ component. Like the $L_e + L_\mu + L_\tau$ case, for small $M_{Z'}$, this model is also strongly constrained by flavor-changing meson decays due to the anomalous $Z'WW$ coupling [38]. The measurement of $K \to \pi \nu \bar{\nu}$ and $B \to K \mu \mu$ decay rates has already excluded the cyan shaded region in Fig. 11. A prospective high-energy electron-positron collider could probe the viable region of Z' masses via the multimuon searches, similar to the limit set by *BABAR* (not shown in Fig. 11 because it is superseded by CCFR) [58].

In view of neutrino cosmology, the gauged $L_\mu + L_\tau$ model has an attractive aspect where the scalars Φ and S both carry $U(1)_\ell$ charge 2. This allows them to directly give Majorana masses to the right-handed neutrinos, which is necessary for being consistent with the ΔN_{eff} bound in cosmology and keeping the Z' sufficiently light, as discussed in Sec. IVB. However, with the minimal particle content given in Table I, the gauged $L_\mu + L_\tau$ model cannot generate realistic active neutrino masses and mixings. This is mainly because the electron neutrino in this model is not charged under the $U(1)_\ell$, which forbids it to mix with the μ and τ flavors unless a charge one scalar (named S') under $U(1)_\ell$, with a nonvanishing VEV, is introduced. The relevant Yukawa interactions, and Majorana mass terms, accounting for realistic neutrino masses and mixings take the form

$$Y_\nu^{ee}\bar{L}_e\tilde{H}\nu_{\mathrm{Re}} + \sum_{\alpha,\beta=\mu,\tau}Y_\nu^{\alpha\beta}\bar{L}_\alpha\tilde{H}\nu_{R\beta} + M_{ee}\bar{\nu}_{\mathrm{Re}}^c\nu_{\mathrm{Re}}$$

$$+ \sum_{\alpha=\mu,\tau}Y_{e\alpha}''S'\bar{\nu}_{\mathrm{Re}}^c\nu_{R\beta} + \sum_{\alpha,\beta=\mu,\tau}Y_{\alpha\beta}'\Phi\bar{\nu}_{R\alpha}^c\nu_{R\beta} + \mathrm{H.c.}, \quad (5.2)$$

where we also have to introduce an electron flavored right-handed neutrino ν_{Re}, which is a $U(1)_\ell$ singlet and can have a bare Majorana mass M_{ee}.

The dark matter phenomenology in the gauged $L_\mu + L_\tau$ model is similar to that discussed in Sec. IV C, except that there could be an additional annihilation channel $\chi\bar{\chi} \to \nu_R\nu_R$ through an s-channel Φ or S exchange, if kinematically allowed, as their $U(1)_\ell$ quantum numbers match for $N_g = 2$. These new annihilation channels introduce additional model dependence in the relic density calculations.

Finally, the contribution to electron EDM in the gauged $L_\mu + L_\tau$ model is suppressed compared to the gauged $L_e + L_\mu + L_\tau$ case, by the absence of Z'-electron coupling.

VI. THE CASE OF GAUGED BARYON NUMBER *B*

In this section we comment on an alternative $U(1)$ extension of the standard model where the new electroweak baryogenesis mechanism proposed in this work could also work. Here we consider gauging the baryon number, $U(1)_B$, instead of the lepton number, under which the SM quarks carry charge $1/3$ but leptons are neutral. An interesting observation is that the same new fermion content as in Table I could also cancel all $U(1)_B$ gauge anomalies, where the L_L', e_R', χ_R, L_R'', e_L'', χ_L fields carry, under $U(1)_B$, the same charges assigned in Table I, Ref. [16].[14] On the other hand, the right-handed neutrinos ν_R^i are now neutral under $U(1)_B$ and they are just introduced for the purpose of giving mass to the neutrinos. An immediate consequence of this setup is that, without participating in the new $U(1)_B$ interactions, the ν_R^i's will not be thermalized in the early Universe. Therefore, unlike the $U(1)_\ell$ case, the Dirac neutrino mass scenario is consistent with the cosmological constraints on ΔN_{eff} in the gauged $U(1)_B$ model.

For electroweak baryogenesis, the baryonic Z_0' background could still be generated from the χ-bubble-wall interaction, which now serves as the baryon number chemical potential for the SM quarks, instead of leptons as in the $U(1)_\ell$ models. As a result, the Boltzmann equation Eq. (3.22) will become directly 1 for the baryon asymmetry, with the replacement $\Delta n_L \to \Delta n_B$, the thermal equilibrium asymmetry Δn_B^{EQ} being identical to Eq. (3.21). It is worth noting that the baryon charge factor $1/3$ for quarks is now compensated by the number of colors. The existing

---

[14]We keep the same notation as for $U(1)_l$, in spite of the fact that these new states carry baryon number. Observe that they are all color singlets.
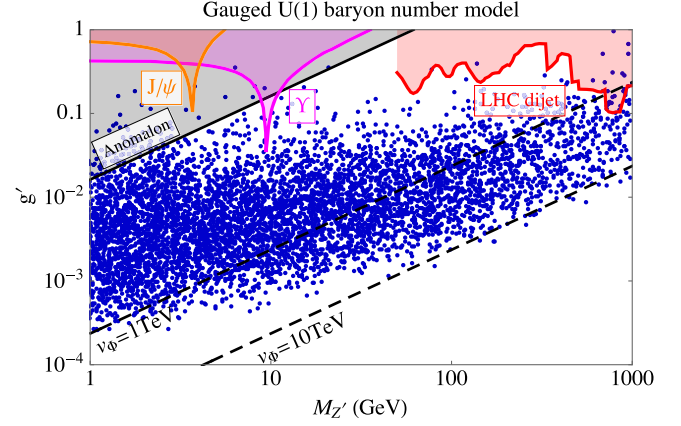

Gauged U(1) baryon number model

FIG. 12. The parameter space of the gauged $U(1)_B$ model that could generate the observed baryon asymmetry of the Universe (blue points), in the $g'-M_{Z'}$ plane. The colorful shaded regions have been excluded by the existing constraints from LHC dijet searches (red), hadronic width of Υ (magenta), and J/Psi (orange). The gray shaded region is the minimally excluded region by the LEP bound on electric charged anomalon fields, assuming their Yukawa couplings with the VEV v_Φ are near the perturbative limit $\sqrt{4\pi}$. The black dashed lines correspond to v_Φ equal to 1 and 10 TeV.

constraints on the baryogenesis viable parameter space are shown in Fig. 12. The baryogenesis viable parameter space in this model is the same as the blue points shown in Fig. 5, except for a different set of experimental constraints on the baryonic Z' [59]. In particular, the LHC constraints on the baryonic Z'-quark coupling is much weaker than the LEP constraint on leptophilic Z' [60]. This allows a wider window for our EWBG mechanism to be successful.

Because the Z' in this case only couples to quarks, the dark sector CP violation dominantly contributes to quark EDMs, instead of the electron EDM, which are less severely constrained.

Like the gauged $U(1)_\ell$ model, here the dark fermion χ could still be a thermal dark matter candidate. Its annihilation channels are similar to those depicted in Fig. 6, except that the annihilation final states are quarks instead of leptons. On the other hand, direct detection constraints become much stronger because in the gauged $U(1)_B$ model the Z' directly couples to quarks and the dark-matter-nucleon scattering now occurs at tree level. For generic values of q of order 1, the current direct detection limit on the spin-independent dark-matter-nucleon scattering cross section implies $v_\Phi \gtrsim 20$ TeV. This constraint is in tension with most of the EWBG favored points in Fig. 12. A possible way to alleviate this tension is to choose $q = -3/2$ in which case the dark-matter-Z' coupling becomes an axial current interaction and the corresponding dark-matter-nucleon scattering is suppressed by the incoming dark matter velocity in the galactic halo.

Analogous to previous cases, because the Z' couples to an anomalous current with respect to $SU(2)_L^2$ in the

low-energy theory, it makes contributions to flavor-changing meson decays such as $K \to \pi Z'$ and $B \to KZ'$ as shown in Ref. [38]. However, in the $U(1)_B$ model the Z' dominantly decays into quarks and antiquarks, while the decay into charged leptons could only occur through a $Z'\gamma$ kinetic mixing, and is subdominant if the kinetic mixing is generated at loop level. As a result, the corresponding flavor-changing constraints are much weaker and do not appear in the range shown in Fig. 12.

VII. CONCLUSION

One of the main challenges to electroweak baryogenesis models is that the required amount of CP violation can be at odds with the improved limits on the electron and neutron electric dipole moments. In this work, we propose a model where electroweak baryogenesis is triggered by a CP violating dark sector. During the electroweak phase transition, the CP violating effect is transferred from the dark to the visible sector at tree level via the background of a Z'_0 gauge boson, whereas at zero temperature the transmission of CPV effects could be suppressed up to four-loop level. This mechanism helps to alleviate the otherwise severe EDM constraints on the viable baryogenesis parameter space.

The $U(1)_\ell$ model we have considered is based on a gauged lepton number symmetry, where the anomaly cancellation condition requires extending the SM sector with new fermions carrying lepton number. The lightest of these fermions plays the role of dark matter. After the spontaneous breaking of the gauged lepton number, once all the new fermion fields (the anomalons)—with the exception of the dark matter candidate—are integrated out, the fermion content of the effective theory contains all SM fermions, right handed neutrinos, and the dark matter. The force carrier of the new gauge interaction, Z', couples to the lepton number current involving all fermions in the effective theory, which is anomalous with respect to $SU(2)_L$, a key ingredient for the baryogenesis mechanism to work.

To achieve a first-order electroweak phase transition we introduce a SM singlet S in the dark sector, which couples to the Higgs boson portal and may allow for a two-step phase transition in the early Universe. Similar studies in the literature have shown that after an initial transition from a trivial vacuum state $(v_S, 0)$ at very high temperatures, it is possible to trigger a strong first-order transition to the electroweak vacuum $(0, v)$, thereby creating the out-of-equilibrium condition necessary for baryogenesis. A detailed analysis of the phase transition history and its relation to the proposed mechanism for electroweak baryogenesis will be presented elsewhere.

The role of the dark sector CP violation in our baryogenesis mechanism for the $U(1)_\ell$ model can be summarized in the following steps:

(1) CP is first violated in the dark sector, containing the $\chi_{L,R}$ fermions. Their mass term has an irreducible phase that becomes time dependent only during the first-order electroweak phase transition, involving both the Higgs field and the dark scalar S, as described above.

(2) This time-dependent CP violating mass generates particle chiral asymmetries for $\chi_{L,R}$ in the dark sector, which diffuse to the exterior of the bubble wall, where SM sphalerons are active.

(3) By model construction, χ_L and χ_R carry different $U(1)_\ell$ charges. As a result, their chiral asymmetries generate a net $U(1)_\ell$ charge density near the wall, which yields a Coulomb background for the Z'_0 gauge field.

(4) Given that the gauge field Z'_0 couples not only to the dark sector leptons but also to the SM leptons, it generates a chemical potential for the SM leptons.

(5) In the presence of sphaleron processes, which are active outside the bubble, the SM lepton number asymmetry evolves towards its equilibrium value set by the above chemical potential.

(6) As sphalerons preserve $B - L$, which originally was 0, they can change the generated SM lepton number into baryon number. Hence, a baryon number asymmetry is equally generated.

(7) Inside the bubbles the sphaleron processes are suppressed, and the baryon asymmetry generated at the phase transition is not washed out. This process sets the baryon asymmetry as an input for the initial condition in standard cosmology.

As for the phenomenology of the present model, the contributions to EDM are highly suppressed, below the present experimental limits, and we do not expect to see a positive signal in the next generation of experiments. Instead, one of our main predictions, in particular, for the $U(1)_\ell$ model, is a leptophilic Z' boson with mass below the TeV scale. The lighter the Z', the more weakly coupled it should be, as shown in Fig. 5. It serves as a very well-motivated target for a number of searches at near future and prospective experiments, such as BELLE II, NA64 (μ mode), and SHiP, as well as a possible Higgs factory.

Accommodating a dark matter candidate within this new EWBG mechanism provides an additional handle in probing this idea. Concerning the fermion candidate χ to dark matter, we show that the annihilation cross sections involving the new force carrier Z' are too small. However the dark matter annihilation into the new scalar S comes to the rescue, yielding the correct relic abundance via thermal freeze-out. Direct detection experiments also yield important information on the parameter space compatible with EWBG. The most relevant, straightforward contribution comes from the Z' exchange, which, given the leptophilic nature of this new gauge boson in the $U(1)_\ell$ model, implies that dark matter scattering occurs at loop

level. Future direct dark matter searches, with an improvement of about 2 orders of magnitude over present bounds, will provide an important test of the viable parameter space in the $U(1)_\ell$ model of EWBG.

Finally, there are novel collider signals from the new additional scalar *S*, which can be pair produced via an s-channel off-shell Higgs boson, or singly produced through mixing with the Higgs boson. The former, pair-production mode could lead to eight charged lepton final states from the decays of the Z' s. The latter, single-production mode, instead, could yield four charged leptons. For both cases, one could reconstruct the Z' mass from the invariant mass of the charged lepton pairs. The new scalar *S* can also be virtually produced via mixing with the Higgs boson, altering the Higgs boson phenomenology. Current bounds on the Higgs boson exotic decays still allow for a large region of parameter space compatible with our EWBG mechanism, and provide interesting opportunities for near-future searches in the Higgs decay to $Z'Z'$ when kinematically allowed.

Similar, corresponding, comments should apply to the $U(1)_B$ model after replacing *L* by *B* and leptons by quarks. However, for the DM candidate χ in the $U(1)_B$ case, already present direct detection constraints make the scenario quite challenging. Nevertheless observe that it is possible for χ to be only a fraction of the total dark matter in the Universe. In that case, the direct detection bounds, as computed here for any of the models, would become less stringent.

APPENDIX A: EQUATION FOR THE LEPTON ASYMMETRY

In this appendix we provide more details about solving the sphaleron rate equation (3.22), to obtain the final lepton/baryon asymmetry. We first rewrite Eq. (3.22) here,

$$\frac{d\Delta n_{L_L}(z,t)}{dt} = \Gamma_{\text{sph}}(z - v_\omega t)[\Delta n_{L_L}^{\text{EQ}}(z - v_\omega t) - \Delta n_{L_L}(z,t)],$$

(A1)

where the sphaleron rate Γ_{sph} was given in Eq. (3.23) for the symmetric and broken phases.

Several remarks are in order here.

(i) We solve Δn_L for a generic point at a distance *z* from the moving bubble wall. We assume that the bubble is formed at an initial time that we arbitrarily fix to $t = 0$. The bubble wall passes through the point *z* at time $t = z/v_\omega$, and turns on the Higgs VEV at this point. We are interested in its final value, i.e., in principle, at $t \to \infty$, after the bubble wall has passed through and bubble nucleation has taken place.

(ii) The electroweak sphaleron rate is strongly suppressed in the broken phase for a strong first-order phase transition, where the Higgs VEV at the tunneling (or nucleation) temperature is $v_n \gtrsim T_n$. This behavior follows since $e^{-M_{\text{sph}}/T_n} \ll 1$, and hence Γ_{sph} at the broken phase is negligible. At point *z*, instead, the sphaleron process is active, and its rate is a constant, i.e., $\Gamma_{\text{sph}}(z - v_\omega t) = \Gamma_0 \neq 0$, for the time window $0 \leq t \leq z/v_\omega$.

(iii) As calculated, and shown in the left panel of Fig. 4, the source term is peaked, and localized, around the moving bubble wall. It is highly suppressed at large instantaneous distance from the wall, i.e., for *z* greater than a few times the wall width L_ω.

To solve Eq. (A1), we first get rid of the damping term on the right-hand side with the redefinition

$$A(z,t) \equiv \Delta n_{L_L}(z,t)e^{\Gamma_0 t}.$$

(A2)

The differential equation for $A(z,t)$ is then

$$\frac{dA(z,t)}{dt} = e^{\Gamma_0 t}\Gamma_0 \Delta n_{L_L}^{\text{EQ}}(z - v_\omega t),$$

(A3)

As explained in the second bullet above, this equation is only valid in the time window $0 \leq t \leq z/v_\omega$, as for larger values of *t*, $\Gamma_{\text{sph}} \simeq 0$. The solution for $A(z,t)$ could be obtained by simply integrating the right-hand side over time, and then we could use Eq. (A2) to compute $\Delta n_{L_L}(z,t)$. For $t = z/v_\omega$, we have

$$\Delta n_{L_L}(z,t)|_{t=z/v_\omega} = \Gamma_0 \int_0^{z/v_\omega} dt' \Delta n_{L_L}^{\text{EQ}}(z - v_\omega t')e^{\Gamma_0(t' - z/v_\omega)}$$

$$= \frac{\Gamma_0}{v_\omega} \int_0^z dy \Delta n_{L_L}^{\text{EQ}}(y)e^{-\Gamma_0 y/v_\omega},$$

(A4)

where in the second step, we have changed the integration variable from t' to $y = z - v_\omega t'$, the coordinate in the bubble wall center-of-mass frame.

Based on the above discussion, after the bubble wall passes through the point z, the Higgs VEV turns on, and the sphaleron process is highly suppressed. Consequently, the quantity Δn_{L_L} is conserved in the broken electroweak phase. In other words, the created baryon/lepton asymmetry freezes in, and we can derive that at $t \to \infty$,

$$\Delta n_{L_L}(z) \equiv \Delta n_{L_L}(z, \infty) \simeq \frac{\Gamma_0}{v_\omega} \int_0^z dy \, \Delta n_{L_L}^{\text{EQ}}(y) e^{-\Gamma_0 y / v_\omega}.$$

$$(A5)$$

Therefore we define the asymmetry of the final lepton density in the Universe, integrating over all points z, as

$$\Delta n_{L_L} = \int_0^\infty dz \frac{d\Delta n_{L_L}(z)}{dz} = \frac{\Gamma_0}{v_\omega} \int_0^\infty dz \, \Delta n_{L_L}^{\text{EQ}}(z) e^{-\Gamma_0 z / v_\omega},$$

$$(A6)$$

which is the result quoted in Eq. (3.24) in the main text. Notice that we are integrating over all points $z > 0$, outside the bubble, as we are assuming that in the interior of the bubble, $z < 0$, $\Gamma_{sph} \simeq 0$.

APPENDIX B: THE CASE OF A NONANOMALOUS $U(1)_\ell \otimes SU(2)_L^2$ EFFECTIVE THEORY

Let us first consider the case where the masses of L_L' and L_R'' doublet fields are much smaller than the critical temperature of the EWPT, and they are not integrated out. The fermionic current $\mathcal{J}^\mu$ that Z' couples to takes then the form

$$\mathcal{J}^\mu = \sum_{i=1}^{N_g} \bar{L}_{L_i} \gamma^\mu L_{L_i} + \mathsf{q} \bar{L}_L' \gamma^\mu L_L' + (\mathsf{q} + N_g) \bar{L}_R'' \gamma^\mu L_R''$$
$$+ \cdots,$$

$$(B1)$$

where L_{L_i} ($i = 1, 2, 3$) are the SM lepton doublets, and the ellipsis represents the terms involving $SU(2)_L$ singlet fields. The current $\mathcal{J}^\mu$ is nonanomalous with respect to the SM $SU(2)_L$, i.e.,

$$\partial_\mu \mathcal{J}^\mu \propto \text{tr}(\ell \tau^a \tau^b) W^a \tilde{W}^b$$
$$\propto [N_g \times 1 + \mathsf{q} - (\mathsf{q} + N_g)] \text{tr}(W\tilde{W}) = 0, \quad (B2)$$

where W ($\tilde{W}$) is the $SU(2)_L$ field (dual field) strength, and the Pauli matrices τ^a are $SU(2)_L$ generators.

Next, we assume the $\langle Z_0' \rangle$ background to be present during EWBG, still generated by the CP violating χ-bubble-wall interaction, given by Eq. (3.19). Through the gauge interactions, the Z_0' background serves as

chemical potential for the fields charged under it, and leads to the thermal equilibrium asymmetry in their number densities. Of particular interest to us are those for the $SU(2)_L$ doublets,

$$\Delta n_{L_L}^{\text{EQ}} = N_g \times 1 \times \frac{2}{3} T_c^2 g' \langle Z_0' \rangle,$$

$$\Delta n_{L_L'}^{\text{EQ}} = 1 \times \mathsf{q} \times \frac{2}{3} T_c^2 g' \langle Z_0' \rangle,$$

$$\Delta n_{L_R''}^{\text{EQ}} = 1 \times (\mathsf{q} + N_g) \times \frac{2}{3} T_c^2 g' \langle Z_0' \rangle. \quad (B3)$$

In the context of EWBG, the electroweak sphaleron processes are responsible for changes in the lepton and baryon numbers in the Universe. In the presence of L_L', L_R'' fields in the thermal bath, they also participate. The actual changes in the particle asymmetries are tied to each other, and satisfy the following relations,

$$\frac{\partial}{\partial t} \Delta n_{B_L} = \frac{\partial}{\partial t} \Delta n_{L_L} = 3 \frac{\partial}{\partial t} \Delta n_{L_L'} = -3 \frac{\partial}{\partial t} \Delta n_{L_R''}, \quad (B4)$$

where B_L denotes the baryon number in left-handed SM doublets. It is useful to define the "effective total lepton asymmetry" as

$$\Delta n_{L,\text{eff}}(z, t) \equiv \Delta n_{L_L}(z, t) + \Delta n_{L_L'}(z, t) - \Delta n_{L_R''}(z, t),$$

$$(B5)$$

so that Eq. (B4) implies

$$\frac{\partial}{\partial t} \Delta n_{B_L}(z, t) = \frac{3}{5} \frac{\partial}{\partial t} \Delta n_{L,\text{eff}}(z, t). \quad (B6)$$

The Boltzmann equation for $\Delta n_{L,\text{eff}}(z, t)$ satisfies

$$\frac{\partial}{\partial t} \Delta n_{L,\text{eff}}(z, t) = \Gamma_{\text{sph}}(z - v_\omega t)$$
$$\times [\Delta n_{L,\text{eff}}^{\text{EQ}}(z - v_\omega t) - \Delta n_{L,\text{eff}}(z, t)],$$

$$(B7)$$

$$\Delta n_{L,\text{eff}}^{\text{EQ}} = \Delta n_{L_L}^{\text{EQ}} + \Delta n_{L_L'}^{\text{EQ}} - \Delta n_{L_R''}^{\text{EQ}}. \quad (B8)$$

Equation (B3) then implies that a cancellation occurs in Eq. (B8), leading to $\Delta n_{L,\text{eff}}^{\text{EQ}} = 0$. In this case, the Boltzmann equation for $\Delta n_{L,\text{eff}}(z, t)$ has no source term, and assuming the Universe begins without any particle asymmetries, no $\Delta n_{L,\text{eff}}$ is generated. In turn Eq. (B6) implies that the baryon asymmetry cannot be generated.

One should note that such a conclusion is drawn by assuming the L_L', L_R'' fields to be relativistic degrees of freedom in the thermal bath during the EWPT. As pointed out in [11], the above cancellation is closely related to

Eq. (B2), the conservation of the current $\mathcal{J}^\mu$, with respect to $SU(2)_L$.

On the other hand, if L'_L, L''_R obtain a sufficiently large $U(1)_\ell$ symmetry breaking mass through the Yukawa coupling to the Φ field as discussed in the main text, their thermal number densities in Eq (B3) become Boltzmann suppressed. In this case, the above cancellation no longer occurs, and the proposed EWBG mechanism could be successful. In the limit when L'_L, L''_R are very heavy and

integrated out, the current that Z' couples to in the low-energy theory becomes

$$J^\mu = \sum_{i=1}^{3} \bar{L}_{L_i} \gamma^\mu L_{L_i} + \cdots, \tag{B9}$$

which is anomalous with respect to $SU(2)_L$. In summary, the created baryon asymmetry should be proportional to the nonconservation of the current J^μ [11], as previously stated.

[1] V. A. Kuzmin, V. A. Rubakov, and M. E. Shaposhnikov, On the anomalous electroweak Baryon number non-conservation in the Early Universe, Phys. Lett. **155B,** 36 (1985).

[2] A. G. Cohen, D. B. Kaplan, and A. E. Nelson, Weak scale Baryogenesis, Phys. Lett. B **245,** 561 (1990); G. R. Farrar and M. E. Shaposhnikov, Baryon Asymmetry of the Universe in the Minimal standard model, Phys. Rev. Lett. **70,** 2833 (1993); Erratum, Phys. Rev. Lett. **71,** 210 (1993); P. Huet and A. E. Nelson, *CP* violation and electroweak baryogenesis in extensions of the standard model, Phys. Lett. B **355,** 229 (1995); Electroweak baryogenesis in supersymmetric models, Phys. Rev. D **53,** 4578 (1996); A. Riotto, Towards a nonequilibrium quantum field theory approach to electroweak baryogenesis, Phys. Rev. D **53,** 5834 (1996); M. Carena, M. Quiros, A. Riotto, I. Vilja, and C. E. M. Wagner, Electroweak baryogenesis and low-energy supersymmetry, Nucl. Phys. **B503,** 387 (1997); M. Carena, J. M. Moreno, M. Quiros, M. Seco, and C. E. M. Wagner, Supersymmetric *CP* violating currents and electroweak baryogenesis, Nucl. Phys. **B599,** 158 (2001).

[3] J. M. Cline, M. Joyce, and K. Kainulainen, Supersymmetric electroweak baryogenesis, J. High Energy Phys. 07 (2000) 018.

[4] M. Carena, M. Quiros, M. Seco, and C. E. M. Wagner, Improved results in supersymmetric electroweak baryogenesis, Nucl. Phys. **B650,** 24 (2003); C. Lee, V. Cirigliano, and M. J. Ramsey-Musolf, Resonant relaxation in electroweak baryogenesis, Phys. Rev. D **71,** 075010 (2005).

[5] J. M. Cline, Baryogenesis, in *Les Houches Summer School —Session 86: Particle Physics and Cosmology: The Fabric of Spacetime Les Houches, France* (2006).

[6] L. Fromme, S. J. Huber, and M. Seniuch, Baryogenesis in the two-Higgs doublet model, J. High Energy Phys. 11 (2006) 038; V. Cirigliano, S. Profumo, and M. J. Ramsey-Musolf, Baryogenesis, Electric dipole moments and dark matter in the MSSM, J. High Energy Phys. 07 (2006) 002; Y. Li, S. Profumo, and M. Ramsey-Musolf, A comprehensive analysis of electric dipole moment constraints on *CP*-violating phases in the MSSM, J. High Energy Phys. 08 (2010) 062.

[7] V. Andreev *et al.* (ACME Collaboration), Improved limit on the electric dipole moment of the electron, Nature (London) **562,** 355 (2018).

[8] J. Baron *et al.* (ACME Collaboration), Order of magnitude smaller limit on the electric dipole moment of the electron, Science **343,** 269 (2014); W. C. Griffith, M. D. Swallows, T. H. Loftus, M. V. Romalis, B. R. Heckel, and E. N. Fortson, Improved Limit on the Permanent Electric Dipole Moment of Hg-199, Phys. Rev. Lett. **102,** 101601 (2009); C. A. Baker *et al.*, An Improved Experimental Limit on the Electric Dipole Moment of the Neutron, Phys. Rev. Lett. **97,** 131801 (2006).

[9] J. Shu and Y. Zhang, Impact of a *CP* violating Higgs Sector: From LHC to Baryogenesis, Phys. Rev. Lett. **111,** 091801 (2013); S. Ipek, Perturbative analysis of the electron electric dipole moment and *CP* violation in two-Higgs-doublet models, Phys. Rev. D **89,** 073012 (2014); M. Jung and A. Pich, Electric dipole moments in two-Higgs-Doublet models, J. High Energy Phys. 04 (2014) 076; T. Abe, J. Hisano, T. Kitahara, and K. Tobioka, Gauge invariant Barr-Zee type contributions to fermionic EDMs in the two-Higgs doublet models, J. High Energy Phys. 01 (2014) 106; Erratum, J. High Energy Phys. 04 (2016) 161; S. Inoue, M. J. Ramsey-Musolf, and Y. Zhang, *CP*-violating phenomenology of flavor conserving two Higgs doublet models, Phys. Rev. D **89,** 115023 (2014); K. Cheung, J. S. Lee, E. Senaha, and P.-Y. Tseng, Confronting Higgcision with electric dipole moments, J. High Energy Phys. 06 (2014) 149; L. Bian, T. Liu, and J. Shu, Cancellations Between Two-Loop Contributions to the Electron Electric Dipole Moment with a *CP*-Violating Higgs Sector, Phys. Rev. Lett. **115,** 021801 (2015); C.-Y. Chen, S. Dawson, and Y. Zhang, Complementary of LHC and EDMs for exploring Higgs *CP* violation, J. High Energy Phys. 06 (2015) 056; K. Fuyuto, J. Hisano, and E. Senaha, Toward verification of electroweak baryogenesis by electric dipole moments, Phys. Lett. B **755,** 491 (2016); M. Jiang, L. Bian, W. Huang, and J. Shu, Impact of a complex singlet: Electroweak baryogenesis and dark matter, Phys. Rev. D **93,** 065032 (2016); N. Blinov, J. Kozaczuk, D. E. Morrissey, and C. Tamarit, Electroweak Baryogenesis from exotic electroweak symmetry breaking, Phys. Rev. D **92,** 035012 (2015); C. Balazs, G. White, and J. Yue, Effective field theory, electric dipole moments and electroweak baryogenesis, J. High Energy Phys. 03 (2017) 030; L. Bian and N. Chen, Cancellation mechanism in the predictions of electric dipole moments, Phys. Rev. D **95,** 115029 (2017); C.-Y. Chen, H.-L. Li, and

M. Ramsey-Musolf, *CP*-violation in the two Higgs Doublet Model: From the LHC to EDMs, Phys. Rev. D **97,** 015020 (2018); C. Cesarotti, Q. Lu, Y. Nakai, A. Parikh, and M. Reece, Interpreting the electron EDM constraint, J. High Energy Phys. 05 (2019) 059; D. Egana-Ugrinovic and S. Thomas, Higgs Boson contributions to the electron electric dipole moment, arXiv:1810.08631; M. J. Ramsey-Musolf, P. Winslow, and G. White, Color breaking Baryogenesis, Phys. Rev. D **97,** 123509 (2018).

[10] J. M. Cline, K. Kainulainen, and D. Tucker-Smith, Electroweak baryogenesis from a dark sector, Phys. Rev. D **95,** 115006 (2017).

[11] M. Carena, M. Quiros, and Y. Zhang, Electroweak Baryogenesis From Dark *CP* violation, Phys. Rev. Lett. **122,** 201802 (2019).

[12] S. M. Barr and A. Zee, Electric Dipole Moment of the Electron and of the Neutron, Phys. Rev. Lett. **65,** 21 (1990); Erratum, Phys. Rev. Lett. **65,** 2920 (1990).

[13] J. F. Gunion and R. Vega, The electron electric dipole moment for a CP violating neutral Higgs sector, Phys. Lett. B **251,** 157 (1990).

[14] J. Wess and B. Zumino, Consequences of anomalous ward identities, Phys. Lett. **37B,** 95 (1971).

[15] P. F. Perez and M. B. Wise, Baryon and lepton number as local gauge symmetries, Phys. Rev. D **82,** 011901 (2010); Erratum, Phys. Rev. D **82,** 079901 (2010).

[16] M. Duerr, P. F. Perez, and M. B. Wise, Gauge Theory for Baryon and Lepton Numbers with Leptoquarks, Phys. Rev. Lett. **110,** 231801 (2013).

[17] P. Schwaller, T. M. P. Tait, and R. Vega-Morales, Dark matter and vectorlike leptons from gauged lepton number, Phys. Rev. D **88,** 035001 (2013).

[18] W. Altmannshofer, M. Carena, and A. Crivellin, $L_\mu - L_\tau$ theory of Higgs flavor violation and $(g-2)_\mu$, Phys. Rev. D **94,** 095026 (2016).

[19] W. A. Bardeen and B. Zumino, Consistent and covariant anomalies in gauge and gravitational theories, Nucl. Phys. **B244,** 421 (1984).

[20] L. Rosenberg, Electromagnetic interactions of neutrinos, Phys. Rev. **129,** 2786 (1963).

[21] P. J. Fox, I. Low, and Y. Zhang, Top-philic Z' forces at the LHC, J. High Energy Phys. 03 (2018) 074.

[22] J. R. Espinosa, T. Konstandin, and F. Riva, Strong electroweak phase transitions in the standard model with a singlet, Nucl. Phys. **B854,** 592 (2012); H. H. Patel, M. J. Ramsey-Musolf, and M. B. Wise, Color breaking in the early Universe, Phys. Rev. D **88,** 015003 (2013); C. Cheung and Y. Zhang, Electroweak cogenesis, J. High Energy Phys. 09 (2013) 002; D. Curtin, P. Meade, and C.-T. Yu, Testing Electroweak Baryogenesis with future colliders, J. High Energy Phys. 11 (2014) 127.

[23] J. de Vries, M. Postma, J. van de Vis, and G. White, Electroweak Baryogenesis and the standard model effective field theory, J. High Energy Phys. 01 (2018) 089.

[24] G. C. Dorsch, S. J. Huber, and T. Konstandin, Bubble wall velocities in the standard model and beyond, J. Cosmol. Astropart. Phys. 12 (2018) 034.

[25] A. G. Cohen, D. B. Kaplan, and A. E. Nelson, Spontaneous baryogenesis at the weak phase transition, Phys. Lett. B **263,** 86 (1991); E. W. Kolb and M. S. Turner, The early Universe, Front. Phys. **69,** 1 (1990).

[26] H. Davoudiasl, R. Kitano, G. D. Kribs, H. Murayama, and P. J. Steinhardt, Gravitational Baryogenesis, Phys. Rev. Lett. **93,** 201301 (2004); H. Davoudiasl, Gravitationally induced dark matter asymmetry and dark nucleon decay, Phys. Rev. D **88,** 095004 (2013).

[27] D. Bodeker, G. D. Moore, and K. Rummukainen, Chern-Simons number diffusion and hard thermal loops on the lattice, Phys. Rev. D **61,** 056003 (2000).

[28] G. D. Moore, Measuring the broken phase sphaleron rate nonperturbatively, Phys. Rev. D **59,** 014503 (1998); R. Zhou, L. Bian, and H.-K. Guo, Probing the electroweak Sphaleron with gravitational waves, arXiv:1910.00234.

[29] N. Aghanim *et al.* (Planck Collaboration), Planck 2018 results. VI. Cosmological parameters, arXiv:1807.06209.

[30] D. Banerjee *et al.* (NA64 Collaboration), Search for Invisible Decays of sub-GeV Dark Photons in Missing-Energy Events at the CERN SPS, Phys. Rev. Lett. **118,** 011802 (2017); J. P. Lees *et al.* (*BABAR* Collaboration), Search for Invisible Decays of a Dark Photon Produced in e^+e^- Collisions at *BABAR*, Phys. Rev. Lett. **119,** 131804 (2017).

[31] M. Tanabashi *et al.* (Particle Data Group), Review of particle physics, Phys. Rev. D **98,** 030001 (2018).

[32] J. Alcaraz *et al.* (DELPHI, OPAL, ALEPH, LEP Electroweak Working Group and L3 Collaboration), A combination of preliminary electroweak measurements and constraints on the standard model, arXiv:hep-ex/0612034.

[33] J. P. Lees *et al.* (*BABAR* Collaboration), Search for a Dark Photon in e^+e^- Collisions at BABAR, Phys. Rev. Lett. **113,** 201801 (2014).

[34] J. D. Bjorken, R. Essig, P. Schuster, and N. Toro, New fixed-target experiments to search for dark gauge forces, Phys. Rev. D **80,** 075018 (2009).

[35] M. Bauer, P. Foldenauer, and J. Jaeckel, Hunting all the hidden photons, J. High Energy Phys. 07 (2018) 094.

[36] H. Davoudiasl, H.-S. Lee, and W. J. Marciano, Muon Anomaly and Dark Parity Violation, Phys. Rev. Lett. **109,** 031802 (2012).

[37] M. Battaglieri *et al.*, US cosmic visions: New ideas in dark matter 2017: Community report, arXiv:1707.04591.

[38] J. A. Dror, R. Lasenby, and M. Pospelov, New Constraints on Light Vectors Coupled to Anomalous Currents, Phys. Rev. Lett. **119,** 141803 (2017); Dark forces coupled to nonconserved currents, Phys. Rev. D **96,** 075036 (2017).

[39] D. d'Enterria, Physics case of FCC-ee: Proceedings, Physics Prospects for Linear and other Future Colliders after the Discovery of the Higgs (LFC15): Trento, Italy, Frascati Phys. Ser. **61,** 17 (2016); C.-S. S. Group, CEPC-SPPC Preliminary Conceptual Design Report. 1. Physics and Detector, Reports No. IHEP-CEPC-DR-2015-01, No. IHEP-TH-2015-01, No. IHEP-EP-2015-01, 2015.

[40] C. D. Carone and H. Murayama, Realistic models with a light U(1) gauge boson coupled to baryon number, Phys. Rev. D **52,** 484 (1995).

[41] A. Hook, E. Izaguirre, and J. G. Wacker, Model independent bounds on kinetic mixing, Adv. High Energy Phys. **2011,** 859762 (2011); B. A. Dobrescu and C. Frugiuele, Hidden

GeV-Scale Interactions of Quarks, Phys. Rev. Lett. **113,** 061801 (2014).

[42] V. Barger, P. Langacker, and H.-S. Lee, Primordial nucleosynthesis constraints on Z' properties, Phys. Rev. D **67,** 075009 (2003); D. K. Ghosh, G. Senjanovic, and Y. Zhang, Naturally light sterile neutrinos from theory of R-parity, Phys. Lett. B **698,** 420 (2011); J. Hamann, S. Hannestad, G. G. Raffelt, and Y. Y. Y. Wong, Sterile neutrinos with eV masses in cosmology: How disfavoured exactly? J. Cosmol. Astropart. Phys. 09 (2011) 034.

[43] K. N. Abazajian and J. Heeck, Observing Dirac neutrinos in the cosmic microwave background, Phys. Rev. D **100,** 075027 (2019).

[44] J. M. Berryman, A. de Gouva, K. J. Kelly, and Y. Zhang, Dark Matter and Neutrino mass from the smallest non-Abelian Chiral dark sector, Phys. Rev. D **96,** 075010 (2017).

[45] A. Atre, T. Han, S. Pascoli, and B. Zhang, The search for heavy Majorana neutrinos, J. High Energy Phys. 05 (2009) 030.

[46] A. Krovi, I. Low, and Y. Zhang, Broadening dark matter searches at the LHC: Mono-X versus Darkonium channels, J. High Energy Phys. 10 (2018) 026.

[47] P. J. Fox, R. Harnik, J. Kopp, and Y. Tsai, LEP shines light on dark matter, Phys. Rev. D **84,** 014028 (2011).

[48] E. Aprile *et al.* (XENON Collaboration), Dark Matter Search Results from a One Tonne × Year Exposure of XENON1T, Phys. Rev. Lett. **121,** 111302 (2018); X. Cui *et al.* (PandaX-II Collaboration), Dark Matter Results From 54-Ton-Day Exposure of PandaX-II Experiment, Phys. Rev. Lett. **119,** 181302 (2017); D. S. Akerib *et al.* (LUX Collaboration), Results from a Search for Dark Matter in the Complete LUX Exposure, Phys. Rev. Lett. **118,** 021303 (2017).

[49] T. A. Chowdhury, M. Nemevsek, G. Senjanovic, and Y. Zhang, Dark matter as the trigger of strong electroweak phase transition, J. Cosmol. Astropart. Phys. 02 (2012) 029; J. M. Cline, K. Kainulainen, P. Scott, and C. Weniger, Update on scalar singlet dark matter, Phys. Rev. D **88,** 055025 (2013); Erratum, Phys. Rev. D **92,** 039906 (2015).

[50] M. B. Wise and Y. Zhang, Stable bound states of asymmetric dark matter, Phys. Rev. D **90,** 055030 (2014); Erratum, Phys. Rev. D **91,** 039907 (2015); Y. Zhang, Long-lived light mediator to dark matter and primordial small scale spectrum, J. Cosmol. Astropart. Phys. 05 (2015) 008; C. Kouvaris, I. M. Shoemaker, and K. Tuominen, Self-interacting dark matter through the Higgs portal, Phys. Rev. D **91,** 043519 (2015).

[51] M. Carena, Z. Liu, and M. Riembau, Probing the electroweak phase transition via enhanced di-Higgs boson production, Phys. Rev. D **97,** 095032 (2018); G. Aad *et al.* (ATLAS and CMS Collaborations), Measurements of the Higgs boson production and decay rates and constraints on its couplings from a combined ATLAS and CMS analysis of the LHC pp collision data at $\sqrt{s} = 7$ and 8 TeV, J. High Energy Phys. 08 (2016) 045.

[52] E. Accomando *et al.*, Workshop on *CP* studies and nonStandard Higgs physics, arXiv:hep-ph/0608079; Y. Chen, R. Harnik, and R. Vega-Morales, Probing the Higgs Couplings to Photons in h->4l at the LHC, Phys. Rev. Lett. **113,** 191801 (2014).

[53] E. Izaguirre and D. Stolarski, Searching for Higgs Decays to as Many as 8 Leptons, Phys. Rev. Lett. **121,** 221803 (2018).

[54] A. M. Sirunyan *et al.* (CMS Collaboration), Search for electroweak production of charginos and neutralinos in multilepton final states in proton-proton collisions at $\sqrt{s} = 13$ TeV, J. High Energy Phys. 03 (2018) 166.

[55] M. Aaboud *et al.* (ATLAS Collaboration), Search for Higgs boson decays to beyond-the-Standard-Model light bosons in four-lepton events with the ATLAS detector at $\sqrt{s} = 13$ TeV, J. High Energy Phys. 06 (2018) 166.

[56] W. Altmannshofer, S. Gori, M. Pospelov, and I. Yavin, Neutrino Trident Production: A Powerful Probe of New Physics with Neutrino Beams, Phys. Rev. Lett. **113,** 091801 (2014).

[57] T. Araki, S. Hoshino, T. Ota, J. Sato, and T. Shimomura, Detecting the $L_\mu - L_\tau$ gauge boson at Belle II, Phys. Rev. D **95,** 055006 (2017).

[58] J. P. Lees *et al.* (*BABAR* Collaboration), Search for a muonic dark force at *BABAR*, Phys. Rev. D **94,** 011102 (2016).

[59] H. An, X. Ji, and L.-T. Wang, Light dark matter and Z' dark force at colliders, J. High Energy Phys. 07 (2012) 182; B. A. Dobrescu and F. Yu, Coupling-mass mapping of dijet peak searches, Phys. Rev. D **88,** 035021 (2013); Erratum, Phys. Rev. D **90,** 079901 (2014); P. Fileviez Prez, E. Golias, R.-H. Li, and C. Murgui, Leptophobic dark matter and the Baryon number violation scale, Phys. Rev. D **99,** 035009 (2019).

[60] A. M. Sirunyan *et al.* (CMS Collaboration), Search for low mass vector resonances decaying into quark-antiquark pairs in proton-proton collisions at $\sqrt{s} = 13$ TeV, J. High Energy Phys. 01 (2018) 097; ATLAS Collaboration, Search for light dijet resonances with the ATLAS detector using a Trigger-Level Analysis in LHC pp collisions at $\sqrt{s} = 13$ TeV, CERN Report No. ATLAS-CONF-2016-030, 2016; A. M. Sirunyan *et al.* (CMS Collaboration), Search for dijet resonances in protonproton collisions at $\sqrt{s} = 13$ TeV and constraints on dark matter and other models, Phys. Lett. B **769,** 520 (2017); Erratum, Phys. Lett. B **772,** 882 (2017); M. Aaboud *et al.* (ATLAS Collaboration), Search for new phenomena in dijet events using 37 fb^{-1} of pp collision data collected at $\sqrt{s} = 13$ TeV with the ATLAS detector, Phys. Rev. D **96,** 052004 (2017).